Report 1993:5

EFFECTS OF REDUCTIONS IN STRATOSPHERIC OZONE ON TROPOSPHERIC CHEMISTRY THROUGH CHANGES IN PHOTOLYSIS RATES

by

J.S. Fuglestvedt[§], J.E. Jonson[*], and I.S.A. Isaksen[§*]

Accepted for publication in *TELLUS*.

[§] CICERO

[*] Institute for Geophysics, University of Oslo

22 November, 1993

EFFECTS OF REDUCTIONS IN STRATOSPHERIC OZONE ON TROPOSPHERIC CHEMISTRY THROUGH CHANGES IN PHOTOLYSIS RATES

by

J.S. Fuglestvedt[§], J.E. Jonson[*], and I.S.A. Isaksen[§ *]

[§] Center for International Climate and Energy Research - Oslo (CICERO), University of Oslo, P.O. Box 1066 Blindern, 0316 Oslo, Norway

[*] Institute for Geophysics, University of Oslo, P.O. Box 1022 Blindern, 0315 Oslo, Norway

ABSTRACT

The observed reductions in stratospheric ozone since the late 1970s are likely to have affected the penetration of UV radiation into the troposphere. We have examined the sensitivity and the response of the tropospheric chemistry to such changes in UV radiation. Based on observations of ozone column densities and model calculations of changes in the ozone column densities after 1970, photodissociation rates for selected years (1970, 1980, 1990, 2000 and 2050) are calculated. These calculations give significant changes in the dissociation rates of some gases, particularly in the dissociation rate for O_3 yielding $O(^1D)$. This increase in photodissociation rates initiates increases in tropospheric OH. However, the model studies show that the OH changes are somewhat damped compared to the changes in short wave radiation due to strong interactions between key species in the troposphere. Ozone is reduced in most areas when the UV radiation increases, but the percentage reductions in ozone are significantly smaller than the percentage UV increases. However, during spring, O_3 increases in regions where NOx is enhanced. The calculations give increased levels of H_2O_2, although the magnitude of the response varies considerably with time of year and with region, and they are largest at high latitudes during spring. The relative changes in methane are found to be less than the relative changes in global average of OH since the largest relative OH changes take place outside the region of most importance for the methane oxidation (low latitudes and low altitudes). In addition, the effect is delayed in accordance with the chemical lifetime of methane (~10 years). The results indicate that increased fluxes of UV due to reduced ozone columns may have contributed to the reduction in the growth rate of methane, and the magnitude of this effect is estimated to ~1/3 of the reduction. It is therefore unlikely that changes in UV fluxes is the main cause of the reduction in the growth rate of methane which has been observed during the 1980s. The mechanism constitutes a negative indirect chemical effect on climate from the ozone depleting substances, mainly the CFCs.

CONTENTS

1. Introduction

The significant ozone column reductions, which have been observed during the last decade (WMO, 1992) and which have been particularly notable the last few years (Gleason et al., 1993), have undoubtedly led to significant increases in the flux of UV radiation into the troposphere. This in turn has certainly had its impacts on tropospheric chemistry. Changes in stratospheric ozone may in this way affect some fundamental chemical processes in the troposphere. Reduced levels of surface O_3 during the years with large reductions of Antarctic stratospheric O_3 have been observed at the South Pole during the austral spring and summer (Schnell et al.,1991). These reductions may be explained by increased fluxes of UV due to reductions in stratospheric ozone (Schnell et al., 1991; Thompson, 1991).

The purpose of this paper is to study the response and the sensitivity in the tropospheric chemistry to changes in stratospheric ozone. We will first focus on the hydroxyl radical (OH) since it is the most important oxidizing compound in the troposphere, responsible for the degradation of hydrocarbons, several halocarbons, sulphur containing species and NOx. Many greenhouse gases are among the components removed by hydroxyl radicals. OH is therefore a central key component that initiates, among other things, the production of tropospheric ozone. Hydrogen peroxide (H_2O_2) is an important oxidant of S^{IV} in the aqueous phase and is also given attention. We will further concentrate on the tropospheric greenhouse gases O_3 and CH_4, which also affect the oxidation processes in the atmosphere. If the observed stratospheric decrease in ozone can be linked to increased CFC released chlorine, as there is increasing evidence of, changes in the levels of tropospheric greenhouse gases from increased UV radiation demonstrate another indirect effect from the CFCs.

The possible effects of reductions in stratospheric ozone on tropospheric chemistry have been considered earlier in several papers. Liu and Trainer (1988) used a box model with fixed concentrations of NOx, non-methane hydrocarbons (NMHC), CH_4 and CO to study the responses in O_3, OH, HO_2 and H_2O_2 in the boundary layer for summer conditions. They found that the response in tropospheric O_3 depends

critically on the NOx levels. In areas with high levels of NOx the levels of tropospheric ozone increased in response to reductions in total ozone. For low NOx conditions the effect was of opposite sign. They also found that the responses in OH, HO_2 and H_2O_2 are almost independent of the NOx levels. Gery (1989) discussed the effects of changes in UV-B radiation on tropospheric air quality, and pointed out that the planned programs for improving air quality could be less effective than anticipated if increases in UV-B take place. Thompson et al. (1989) used a one-dimensional model to study the effects of stratospheric ozone depletion on tropospheric levels of O_3, OH and H_2O_2 and the sensitivities of the responses. The model simulates different conditions and regions, and it was found that tropospheric ozone increased in urban regions while reductions were obtained elsewhere. The levels of OH and H_2O_2 were found to increase in response to increased UV in all regions. Jonson and Isaksen (1991) calculated the effects of a 30% reduction in total O_3 in a two-dimensional zonal model, with similar results for tropospheric O_3, OH and H_2O_2. Madronich and Granier (1992) estimated the effect of the observed reductions in total ozone between 1979 and 1989 on the rate of the photolysis of O_3 that initiates the production of OH. They presented their estimated trend for this photolysis rate as a first order estimate of the OH trend, and proposed that the changes in OH may explain a substantial portion of the observed reduction in the growth rate of methane. In Madronich (1993) the responses in tropospheric chemistry to UV changes were discussed and an overview of the reactions and processes controlling the responses was given.

2. Important reactions in the chemistry of the troposphere

Photodissociation of O_3 in the troposphere yielding $O(^1D)$;

$$O_3 + h\upsilon\ (\lambda \leq 320\ nm) \rightarrow O(^1D) + O_2 \qquad J_B(O_3) \qquad R1$$

is very sensitive to changes in the overhead O_3 column. This photolytic reaction triggers a sequence of reactions essential to the oxidation processes in the troposphere.

Enhanced $O(^1D)$ production through R1 leads to an instantaneous increase in OH production in the troposphere when $O(^1D)$ reacts with water vapour:

$$O(^1D) + H_2O \rightarrow OH + OH \qquad R2$$

This reaction is the main source of OH radicals throughout the troposphere. In this way changes in stratospheric ozone will affect the production of tropospheric OH. However, the amplitude of the OH change in response to a change in $O(^1D)$, will to some extent be determined by other chemical reactions since the OH perturbation will initiate responses in the highly intertwined chemistry.

Most of the OH produced (~70 %) reacts with CO:

$$CO + OH \rightarrow CO_2 + H \qquad R3$$

In addition, a significant fraction of the OH radicals reacts with CH_4:

$$CH_4 + OH \rightarrow CH_3 + H_2O \qquad R4$$

In both cases, HO_2 is formed through further reactions (see appendix A). OH is reformed when HO_2 reacts with NO or O_3:

$$HO_2 + NO \rightarrow OH + NO_2 \qquad R5$$

$$HO_2 + O_3 \rightarrow OH + 2O_2 \qquad R6$$

The above set of reactions establish a rapid equilibrium between OH and HO_2 in the troposphere. Changes in OH will therefore immediately lead to changes in HO_2 and increased levels of OH will lead to increased levels of HO_2. The ratio between OH and HO_2 may, however, change as a result of changes in O_3, CO, CH_4, NO and NO_2. The strong coupling between OH and HO_2 is of importance for OH perturbations since a major part of the loss of odd hydrogen ($HOx = OH + HO_2$) in the free troposphere

proceeds via reactions involving both OH and HO_2:

$$OH + HO_2 \rightarrow H_2O + O_2 \qquad R7$$

or through the sequence

$$HO_2 + HO_2 \rightarrow H_2O_2 + O_2 \qquad R8$$

$$H_2O_2 + OH \rightarrow H_2O + HO_2 \qquad R9$$

or

$$H_2O_2 \rightarrow \text{heterogeneous removal or dry deposition} \qquad R10$$

In addition, HOx may be lost during the oxidation of methane in NOx poor environments through reactions between CH_3O_2 and HO_2 (Crutzen, 1987).

Since a major part of the loss of HOx in the free troposphere proceeds via reactions involving both OH and HO_2, the overall loss rate of odd hydrogen (and thereby the loss of OH) is affected by the perturbation in the chemistry initiated by the changes in OH.

The OH production is also likely to be affected by changes in ozone levels. R5 leads to production of O_3 since NO_2 will rapidly be photolyzed to give O_3. These reactions constitute a source of ozone since the oxidation of NO to NO_2 takes place without consumption of O_3. Reaction R6, on the other hand, is a direct sink of O_3. It is therefore essential to the ozone budget which of the two reactions that dominates. Due to the low levels of NO in the background troposphere, R6 dominates over R5 in most of the troposphere. In regions with high NO levels, reaction R5 dominates (Crutzen, 1987; Liu and Trainer, 1988). If O_3 is reduced (for instance by R6), less O_3 will be available for photolysis (R1) and subsequent production of OH through R2.

In regions strongly affected by pollution, with high NOx levels, a significant loss of odd hydrogen may also take place through the reaction (M is an air molecule):

$$NO_2 + OH + M \rightarrow HNO_3 + M \qquad R11$$

This reaction is followed by heterogeneous removal of HNO_3, with only a small fraction being photolyzed back to OH and NO_2.

We have only discussed a few of the major reactions to illustrate the highly non-linear response in the chemistry that can be expected from increased production of OH. A discussion of the impact of the full chemical scheme is given in chapter 6. References for the chemical reactions and rate constants are given in appendix A.

3. Calculations of photodissociation rates

Vertical ozone distributions are calculated with a global two-dimensional (2D) chemistry/transport model extending from ground level to 50 km. The 2D model is run with heterogeneous chemistry between the gaseous phase and polar stratospheric clouds (PSCs) and background particles. For a description of the model see Stordal et al. (1985), Isaksen and Stordal (1986) and Isaksen et al. (1990). These calculated profiles are scaled to match monthly averaged observed total ozone columns as given by Dütsch (1974) representing the levels in 1970, which we take as our reference year.

Time dependent calculations with the same 2D model are then performed to obtain changes in ozone column densities between 1970 and the years 1980, 1990, 2000 and 2050. Different sets of J-values are then calculated for 1970 and the abovementioned following years with a separate model (see description below) and these values are used as input to the 2D tropospheric chemistry model. The stratospheric 2D chemistry model does include a simplified tropospheric chemistry, which to some extent, take into account the effects of changes in tropospheric O_3 on the J-values. Although this constitutes some inconsistency in the calculations, it will only have a small effect on

the J-values. For the years 1980, 1990, 2000 and 2050, J-values are calculated with ozone columns scaled by the calculated changes from the reference year 1970. We have found that the incoming UV flux to the troposphere is controlled by the overlying ozone column rather than the vertical distribution. For intermediate years (i.e. 1971, 1972, etc.) a linear interpolation between the nearest two sets is performed.

Solar fluxes are calculated with an algorithm similar to the one described by Isaksen et al. (1977) with the modifications given in Jonson and Isaksen (1991). The fluxes are calculated according to Beer's law in the wavelength regime 185 - 735 nm. The optical depth for a height interval is determined by absorption by O_2 and O_3, and by scattering by air molecules (Rayleigh scattering), by cloud droplets and by aerosols. Above 50 km scattering is negligible, and is therefore omitted. For scattering of direct radiation a distinction is made between direct and diffuse scattering, where direct denotes scattering along the direction of the incoming beam, whereas diffuse denotes scattering in any arbitrary direction. Both diffuse and direct scattering are subdivided into a forward and a backward mode. For Rayleigh scattering of direct radiation we assume that 80% of the scattering is diffuse, and that scattering is equally distributed between forward and backward mode. For Mie scattering (particles and cloud droplets) more energy is scattered in a forward direction. Furthermore, as the particle size increase, so does forward scattering (Iqbal, 1983). In the solar flux calculations, Mie scattering is assumed to be mostly forward, and more so for cloud droplets than for aerosols. For diffuse scattering and surface reflection the scattering media is assumed to act as a lambertian surface (i.e. the scattering is equally efficient in all directions). Solar fluxes are calculated for every kilometer outside clouds. Within or below clouds, the vertical increments are divided by 12. To account for interactions between the levels, 50 iterations are performed. The albedo of the Earth's surface is kept constant at 0.1. Sensitivity tests have shown that variations in this parameter have negligible effects on the calculated J-values.

Based on the solar fluxes, photodissociation rates (J-values) for altogether 16 of the species included in the chemical scheme are calculated by the equation:
where n denotes specie number, i height level and λ wavelength. $F(\lambda)$ is the actinic

$$J_n^i = \int_{\lambda_1}^{\lambda_2} F_i(\lambda)\sigma(\lambda,T)\phi(\lambda,T)d\lambda \qquad (1)$$

solar flux calculated for the wavelength λ as described above. $\sigma(\lambda)$ is the absorption cross section, and $\phi(\lambda)$ the quantum yield. λ_1 and λ_2 give the interval of wavelengths for which photodissociation rates are calculated (185 -735 nm). For absorption cross sections and quantum yields the recommendations by DeMore et al. (1985), and DeMore et al. (1992) are followed.

Monthly (for the 15th of every month) J-values are calculated for every 10 degree latitude. Climatological averages are applied for the vertical distribution of clouds, cloud types, optical thickness and zonal cloud fractions (Lelieveld et al., 1989; Henderson-Sellers and McGuffie, 1987). Penetration of solar fluxes into the troposphere in the lower part of the spectrum (below approximately 330 nm) is to a large extent determined by the thickness of the ozone column above. For longer wavelengths, the solar fluxes are almost entirely determined by scattering processes. Thus, changes in total O_3 will mainly affect J-values in the UV-B region.

4. Description of the 2D tropospheric chemistry model

To study the chemical responses to changes in the photolysis rate for reaction R1, $J_B(O_3)$, and in the photodissociation rates for 15 other species, a 2D tropospheric chemistry/transport model is used. The model is zonally averaged with a meridional resolution of 10 degrees and a vertical resolution of 0.5 km below 3.25 km and 1.0 km above, up to 16.25 km. The results presented here are calculated with a version using advective winds from Newell et al. (1972) and diffusion coefficients from Hidalgo and Crutzen (1977), with some small modifications (see also Isaksen and Hov, 1987). The numerical scheme for advection, given by Smolarkiewicz (1983), is an upwind scheme with corrective steps to reduce implicit numerical diffusion. Meteorological data are seasonally averaged. The photodissociation rates have a diurnal variation (calculated each hour), and the J-value sets are changed each month. The chemistry is gas-phase

with first order heterogeneous scavenging of soluble species by rain and clouds and sticking on aerosols included. The chemistry scheme is divided into two parts. In the first part, which is used during the first day of each month, all chemical compounds (49) are calculated, with a one hour time step. At the same time, diurnally averaged production and loss terms are calculated based on the diurnal calculations. These averaged terms are then used for the remaining days of the month with a time step of one day in the calculations of the diurnally averaged concentrations. In this way the model resolves the diurnal variation in the concentrations of the short-lived species due to the diurnal variation in the photolysis rates, and thereby derives properly diurnally averaged production and loss terms, which are important due to the non-linear terms in the chemical production and loss terms.

The chemistry scheme is updated according to the latest compilations. The full set of chemical reactions with rate constants and references are given in appendix A. The formation of organic nitrates from reactions between peroxy radicals and NO is included in the chemical scheme. The formation of nitrates increases with the number of carbon atoms in the peroxy radicals and with pressure, while it decreases with increasing temperature. It as assumed that the organic nitrates are stable end products, as suggested by Finlayson-Pitts and Pitts (1986), and that they are removed from the atmosphere by scavenging and/or deposition. Thereby this mechanism forms an additional sink for NOx. A full PAN (peroxyacetylnitrate) chemistry is included in the scheme. This is of importance since PAN forms a reservoir species for the key component NOx. The stability of PAN increase with decreasing temperature. It may therefore transport NOx over large distances and release NOx in regions of the atmosphere where the NOx levels are low.

The numerical integration procedure applied to solve the set of time-dependent differential equations deduced from the chemical reaction scheme, is the quasi steady state approximation (QSSA) method described by Hesstvedt et al. (1978).

Table 1 and 2 give the emissions of NOx, CO, CH_4 and NMHC that is applied in the reference model calculations (Isaksen and Hov, 1987; Berntsen et al., 1989; Isaksen et

al., 1989; WMO , 1992, and references therein).

Table 1. Source strengths of NOx used in the reference calculations (TgN/yr).

Ground sources	37
Lightning	6
Flux from the stratosphere (incl. HNO_3)	0.9
Airplanes	0.7

Table 2. Emissions of CO and hydrocarbons (Tg/yr).

CO	1330
CH_4	608
C_2H_4	33
C_2H_6	20
C_3H_6	17
n-C_4H_{10}	20
m-xylene	10
n-C_6H_{14}	10
Isoprene	195

In the steady state calculations (section 6.1) the initial global level of CH_4 is set equal to 1.7 ppmv (parts per million by volume) and a global CH_4 emission of 608 Tg/yr is applied. In the time-dependent calculations (section 6.2) the initial global level is set equal to 1.4 ppmv (Khalil et al., 1989) with a corresponding methane emission of 533 Tg/yr. The global annual average flux of ozone from the stratosphere is $7.4 \cdot 10^{10}$ molecules/s cm^2 which was calculated with the stratospheric 2D model. Deposition velocities for 6 components (O_3, HNO_3, NO_2, PAN, CO and H_2O_2) are included and have been updated. Appendix B gives the deposition velocities for land, sea and snow/ice, with references.

The fully interactive gas phase chemistry in the model allows us to study how the changes in J-values propagate to generate responses in the different species. This is of fundamental importance when we consider species as O_3, OH, CH_4 and H_2O_2. For further description of the model and examples of its application, see Isaksen et al. (1985), Isaksen and Hov (1987), Berntsen et al. (1992) and Fuglestvedt et al. (1993).

5. Calculated changes in stratospheric ozone and in photolysis rates

The time dependent calculations of the ozone column densities for 1980 and 1990 are based on reported emission data for gases affecting stratospheric ozone. The calculated ozone columns for the year 2050 are based on scenario A described at page 8.12 in WMO (1992). For the year 2000 the scenario is adjusted to take into account the accelerated phase out of the ozone depleting substances which is expected to occur as a result of the agreement that was reached in Copenhagen in December 1992 by the parties to the Montreal Protocol. Table 3 gives the calculated upper stratospheric levels of total inorganic chlorine (Cl_y = Cl + ClO + OHCl + $ClONO_2$ + HCl) in ppbv (parts per billion by volume) for the considered years.

Table 3. Levels of total inorganic chlorine (Cl_y) in the upper stratosphere calculated by the 2D model.

	1970	1980	1990	2000	2050
Cl_y (ppbv)	1.2	1.6	2.5	3.4	2.0

The calculated reduction in global annually averaged total O_3 is 1.5 % for the period 1970 to 1980. In 1990, the calculated reduction is 4.5 % relative to 1970. While the reductions for this year are between approximately 2 and 4 % at lower latitudes, the reductions are 4-8 % at middle latitudes and up to 14 and 20% in the spring months at higher Northern and Southern latitudes, respectively. Comparison of the modelled changes in total ozone between 1980 and 1990 with observations given in WMO (1992) shows that the model reproduces the changes at middle latitudes and high Northern latitudes well, but that the model underestimates the trends at high Southern latitudes in the spring months. This underestimate, is, however, limited in space and time. The calculated reduction in global total O_3 between 1980 and 1990 of 3.1 % is in good agreement with the observed trend of 2.7±1.4 %/decade for the region 65°S to 65°N during the period 1979-1991 (Gleason et al., 1993, and references therein).

The maximum calculated reductions take place in year 2000 when the reduction in total column densities is 4 % at lower latitudes (compared to 1970), but reach 22 % at high Northern latitudes and 30 % at high Southern latitudes. Due to reduced Cl_y after 2000, the calculated ozone column densities are significantly higher in 2050 than in 2000. In fact, they are close to the 1970 levels although the stratospheric level of total inorganic chlorine is larger in 2050 than in 1970. This is due to an assumed increase in methane. There are also changes in the latitudinal distribution. Between 40°N and 60-80°S depending on season, the ozone column densities are slightly thicker than in 1970 (up to ~1.5 %) while at higher latitudes ozone is reduced (less than ~4 %).

The calculated percentage increases in the noon values of the photodissociation rate

for O_3 yielding $O(^1D)$, $J_B(O_3)$, for 1990 relative to 1970 are shown in Figure 1 for the lowest level in the model (250 m). The percentage increases in $J_B(O_3)$ are substantially larger than the corresponding reductions in total ozone.

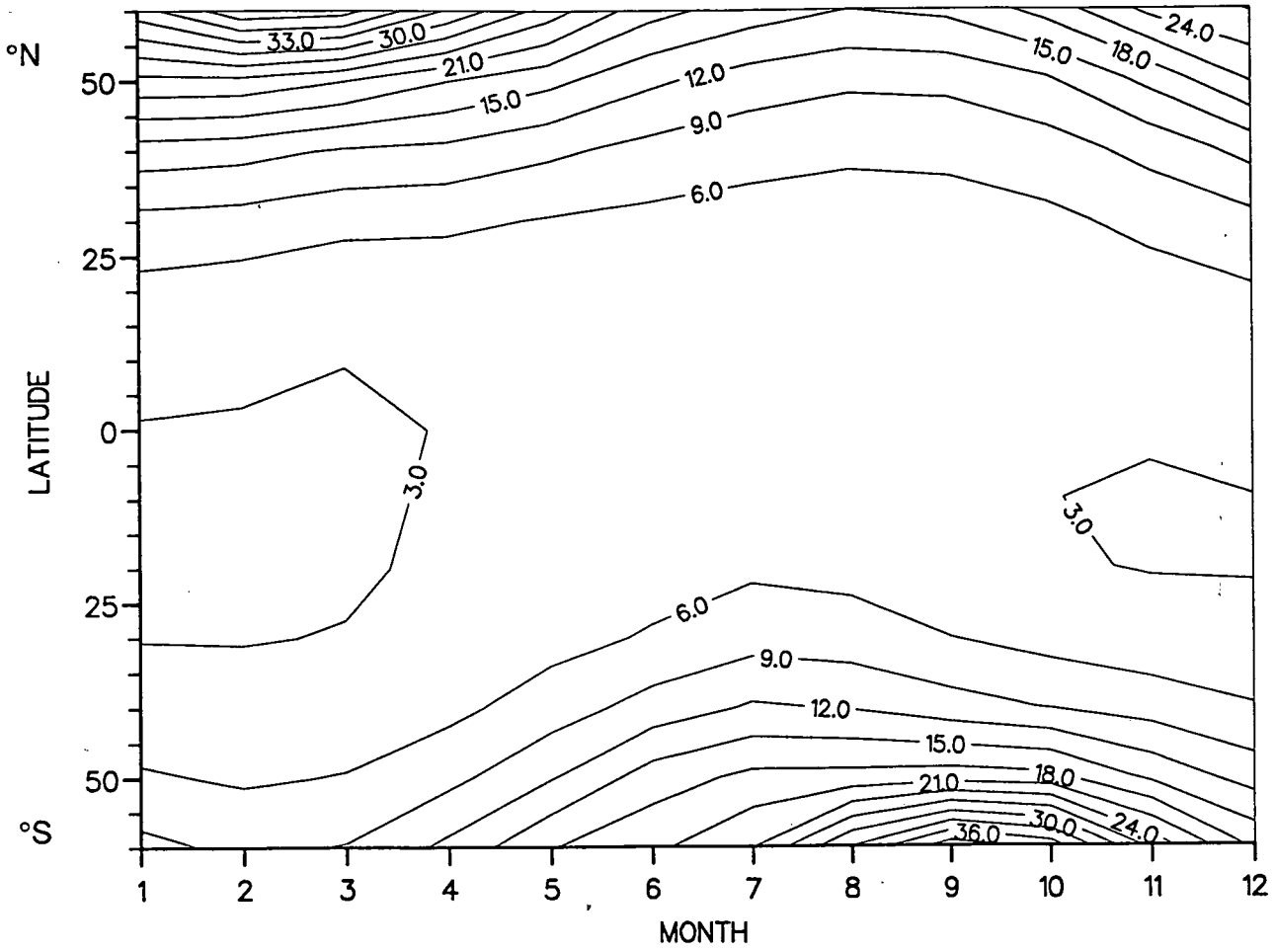

Figure 1. Calculated percentage changes in noon values of $J_B(O_3)$ between 1970 and 1990 in the lowest model layer (250 m).

The calculated increases in the other J-values are smaller than the increases in $J_B(O_3)$. This is illustrated in Table 4 which gives changes in the global annual tropospheric mean values of $J_B(O_3)$, $J(NO_2)$, $J(H_2O_2)$, $J(HNO_3)$, $J_A(CH_2O)$, $J_B(CH_2O)$ for the period 1970 to 1990. The changes in noon values for June at 50°N and altitude level 750 m are also given. Table 5 gives the photolytic reactions for the different species.

Table 4. Percentage changes between 1970 and 1990 in J-values for some important photolytic reactions.

	$J_B(O_3)$	$J(NO_2)$	$J(H_2O_2)$	$J(HNO_3)$	$J_A(CH_2O)$	$J_B(CH_2O)$
June, 50°N, 750 m, noon	12.7 %	0.3 %	2.6 %	7.3 %	3.1 %	1.0 %
Global annual average	6.3 %	0.2 %	1.6 %	4.0 %	2.1 %	0.7 %

Table 5. Photolytic reactions considered in Table 4.

$O_3 + h\nu \rightarrow O(^1D) + O_2$	$J_B(O_3)$
$NO_2 + h\nu \rightarrow NO + O(^3P)$	$J(NO_2)$
$H_2O_2 + h\nu \rightarrow OH + OH$	$J(H_2O_2)$
$HNO_3 + h\nu \rightarrow NO_2 + OH$	$J(HNO_3)$
$CH_2O + h\nu \rightarrow CHO + H$	$J_A(CH_2O)$
$CH_2O + h\nu \rightarrow CO + H_2$	$J_B(CH_2O)$

The numbers show that the changes in the global annual averages are quite small, whereas the changes at 50°N latitude in June are substantially larger. At this time of the year the chemical activity is high and changes in the J-values may then have significant impacts on the chemistry. As Figure 1 shows, the percentage changes in $J_B(O_3)$ can be higher than in June at 50°N latitude, but this is confined to limited regions, and periods of the year, with relative low chemical activity.

6. Responses in tropospheric chemistry: Results and discussions

Firstly, a series of steady state experiments with constant emissions (see Table 1 and 2) are performed. This will demonstrate what the full effects of perturbed UV radiation will be if the perturbations are allowed to work at constant levels over a longer period of time. Secondly, two time dependent experiments are performed: First, the methane emissions are increased, while the UV fluxes and J-values represent 1970 conditions (case A). Then the same rate of increase in the methane emissions is applied, but now the J-values are allowed to change over time in accordance with the modelled changes in total ozone (case B). In all calculations an interactive chemistry is applied. The difference between the cases in the calculated growth rates for methane may be compared to the observed changes in this rate to elucidate the importance of reductions in total ozone.

6.1 Steady State responses

Separate model runs with J-values representing 1970, 1980, 1990, 2000 and 2050 conditions are made. In each case the model is run for 40 years to reach steady state. The following expression is used for the sensitivities of the tropospheric responses:

$$\alpha_X = - \frac{\frac{\Delta X}{X}}{\frac{\Delta \Sigma O_3}{\Sigma O_3}} \qquad (2)$$

X is the global tropospheric annual average level of $J_B(O_3)$, OH, CH_4 or tropospheric ozone. ΣO_3 is total ozone column. ΣO_3 and X represents the reference levels (1970 levels), while ΔX and $\Delta \Sigma O_3$ represents the difference between the perturbed levels (1980, 1990, 2000 or 2050) and 1970 levels for $J_B(O_3)$, OH, CH_4, and tropospheric ozone, and for total ozone, respectively. Percentage changes in global average total ozone and the corresponding α-values for the different perturbations are given in Table 6.

Table 6. Calculated changes in global average O_3 and corresponding changes in the α values for $J_B(O_3)$, OH, CH_4, and O_3 in the troposphere (equation 2).

J-values for year	$\Delta\Sigma O_3 / \Sigma O_3$ (%)	$\alpha_{J_B(O_3)}$	α_{OH}	α_{CH_4}	$\alpha_{trop.O_3}$
1980	-1.46	1.36	1.09	- 0.80	- 0.27
1990	-4.51	1.40	0.89	- 0.78	- 0.32
2000	-6.50	1.41	0.98	- 0.76	- 0.31

The relative changes in the *global tropospheric annual average* value of $J_B(O_3)$ are approximately 40 % larger than the relative changes in total ozone. The relative changes in OH, however, are smaller than the relative changes in $J_B(O_3)$ and approximately of the same magnitude as the relative changes in ozone column densities. The fact that $\alpha_{OH} < \alpha_{J_B(O_3)}$ indicates that there must be chemical mechanisms damping the perturbations of the chemistry from changes in J-values. The effect of increased OH production through R1 and R2 are modified by the responses in several other species and reactions rates.

Reduced ozone column densities lead to reduced tropospheric levels of CH_4 and O_3. The response in methane is somewhat smaller than the response in OH since the largest relative changes in OH occur at high latitudes in the spring months, whereas the lower tropical and subtropical atmosphere, where the relative OH changes are moderate, is the most important region for the methane oxidation. The responses in global average O_3 are significantly smaller than the responses in OH (25-36 %). In the background troposphere the calculated relative changes in OH and O_3 are of the same magnitude, but of opposite signs. This is a result of the reactions R1 and R2, followed by HO_2 produced from R3, and O_3 lost when HO_2 reacts with O_3 through R6. In regions with higher levels of NO, the net O_3 loss is reduced due to the increased importance of R5. In polluted regions in some periods, the ozone producing reaction R5 dominates, which leads to a net production of O_3.

The damping effect on OH may be explained by some simple considerations. The calculations show that the changes in HO_2 generally follow the changes in OH and that the $[OH]/[HO_2]$ ratio is not changed significantly when the J-values are changed.

We assume that the loss of odd hydrogen proceeds predominantly through reaction R7 and R8, and that the fraction of the H_2O_2 produced in R8 that reacts further through R9 and R10 is f. The fraction f is then defined as: $f = a / (a + b)$, where a is the loss of H_2O_2 through R9 and R10, and b is the loss through other reactions (i.e. photolysis of H_2O_2). HOx (OH + HO_2) can be considered to be in steady state:

$$\text{Production} = \text{Loss} = 2 \cdot k_7 \cdot [OH] \cdot [HO_2] + 2 \cdot f \cdot k_8 \cdot [HO_2] \cdot [HO_2]$$

Since $[OH] / [HO_2] \approx c$, the production rate P may be expressed as:

$$\begin{aligned} P &= (2 \cdot k_7 / c) \cdot [OH]^2 + 2 \cdot f \cdot k_8 \cdot ([OH] / c)^2 \\ &= \{(2 \cdot k_7 / c) + (2 \cdot f \cdot k_8) \cdot (1/c^2)\} \cdot [OH]^2 \\ &= \beta \cdot [OH]^2 \end{aligned}$$

which implies that

$$[OH] = (P / \beta)^{1/2}$$

If odd hydrogen is lost only through the reactions R7-R10 and the ratio $[OH]/[HO_2]$ remains constant, as assumed above, we might expect that the changes in OH would equal the square root of the changes in P. In parts of the background troposphere such an assumption seems to be valid. However, in polluted regions where a significant part of the odd hydrogen loss occurs via reaction R11, there are deviations from a square-root relationship. The result is that the changes in global average OH are somewhat larger than the relationship above implies. In addition, changes in tropospheric O_3 will affect the production of OH through reaction R1. When the levels

of NO are very low, HOx may also be lost during the oxidation of methane (Crutzen, 1987). The relations above, however, are only meant for illustrative purposes, and do not take into account all the chemical mechanisms in the model.

6.2 Time-dependent responses

Due to the large time constant for CH_4, it may also be of interest to perform time-dependent calculations. This will show the significance of the time-lags in the system. Model runs for the time period 1970 to 2050 are performed with steady state levels for 1970 as starting conditions. (The emission of methane are adjusted to give a global methane level of 1.4 ppmv at steady state (Khalil et al., 1989). The calculated fields for all chemical components are then used as initial conditions in the model runs.) In the reference run (case A), with an increase of 0.7 %/yr in the methane emissions, but with no long term changes in UV, the model give ~1 %/yr increase in the global mean concentration of methane. The larger relative increase in concentration than in emissions may be attributed to the feedback between CH_4 and OH (Sze, 1977; Isaksen and Hov, 1987; Isaksen, 1988; Valentin, 1991; Isaksen et al., 1992; Berntsen et al., 1992). In the second model run (case B) with the same growth rate in methane emissions, but with long term changes in J-values, we adopt a linear interpolation between the calculated J-value sets for 1970, 1980, 1990, 2000 and 2050.

As Figure 2 shows, the calculated growth rates in the global level of methane start out with ~14 ppbv/yr in both cases. Whereas the rate increases monotonically to 31 ppbv/yr in 2050 in case A, the rate in case B decreases slightly during the first two decades, reaching a minimum of 13.6 ppbv/yr in 1989. After that it increases towards 34 ppbv/yr in 2050. Figure 2 also shows the difference between the growth rates in the two cases (in ppbv/yr). The difference increases most markedly between 1980 and 1990, when the change in stratospheric ozone is largest. The difference increases only slightly between 1990 and 2000 when it reaches a maximum of 3.3 ppbv/yr. After year 2000, the difference in growth rate decreases, and in year 2015 the difference is negative, which means that in the perturbed case the growth rates are larger than in

the case with no perturbation in UV. This is due to the reductions in $J_B(O_3)$ taking place in response to the build up of stratospheric ozone.

In 1990 the global average mixing ratio of CH_4 is ~30 ppbv lower in case B than in case A. This difference reaches a maximum in year 2013 when the mixing ratio of CH_4 is ~80 ppbv lower in the case with changing UV radiation.

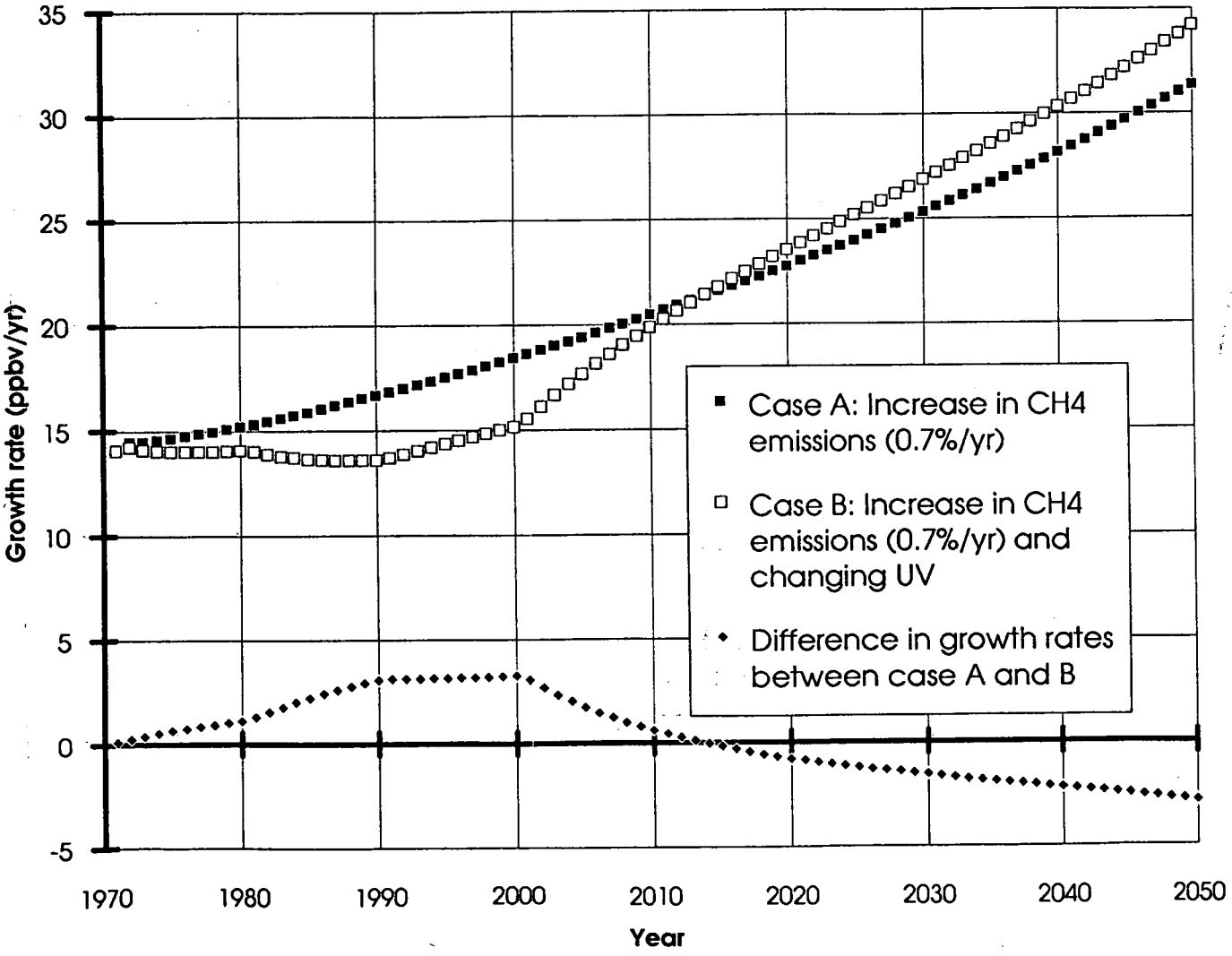

Figure 2. Growth rates of CH_4 (ppbv/year) in case A and B and the difference in growth rate between case A and B as functions of time.

Observations show that the rate of increase of methane has slowed down during the last decade. According to the observations referred to in WMO (1992), the rate of increase was about 18-20 ppbv/yr in 1980, while in 1990 it was about 12-14 ppbv/yr. In Table 7 we show the observed reductions in growth rates for the period 1980-1990 together with the calculated reduction that may result from increased fluxes of UV.

Table 7. Calculated reductions in growth rate of methane during the period 1980-1990 (ppbv/yr) compared to the observed reductions (WMO, 1992).

Observed	Calculated from changes in UV
~ 6 ppbv/yr	2 ppbv/yr

The reductions in total ozone and the accompanying increase in UV and OH, may have contributed to the reduced growth rate, but can not explain the entire reduction.

The gases we focus on have lifetimes that span over a wide range. For OH the lifetime is less than one second, for ozone in the free troposphere it is ~100 days depending on season and region, while for methane it is ~10 years. One may therefore expect large differences in the timing of the responses to changes in total ozone, particularly between OH and CH_4. In Figure 3 the ratio between the global annual averages of total O_3, $J_B(O_3)$, OH, CH_4 and tropospheric O_3 in case B and case A are plotted as functions of time. The figure shows that the global levels of O_3 and OH respond in the same year as the changes in total ozone and J-values take place. The responses in tropospheric O_3 are, however, generally delayed by some weeks relative to when the largest reductions in stratospheric O_3 take place. The maximum response in CH_4 levels is delayed by ~10 years.

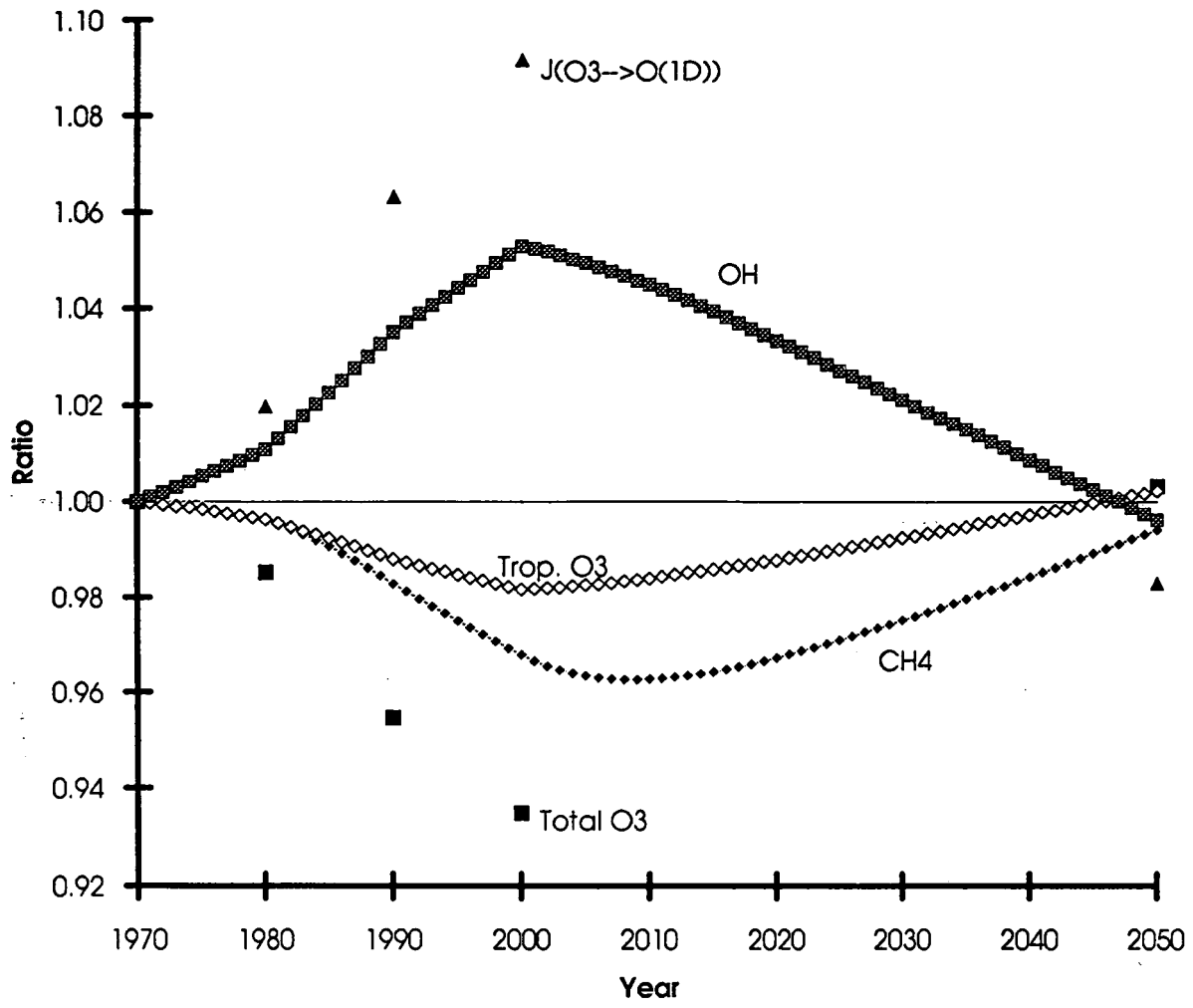

Figure 3. The ratio between the levels in total O_3, $J_B(O_3)$, CH_4, and tropospheric O_3 in case B and A as function of time.

Madronich and Granier (1992) estimated the effect of the observed reductions in total ozone between 1979 and 1989 on $J_B(O_3)$ and found a global average increase of about 4.0±2.8 %/decade which is comparable to our model-based estimate of 4.2 %/decade for the period 1980-1990. Madronich and Granier (1992) assumed that the global average levels of OH and $J_B(O_3)$ are proportional and they presented the estimated

increase in $J_B(O_3)$ as a first-order estimate of the changes in OH. When they applied this OH trend to the global average CH_4 level they estimated a reduction in the growth rate of CH_4 of 6.8±4.8 ppbv/yr. This is substantially larger than our estimate. There are important differences between the approaches in their and our study. While their calculations are based on observed reductions in total O_3, we have used model-derived reductions, although, as we have pointed out, the reductions are comparable. A more significant difference is probably that we have used a 2D model of tropospheric chemistry and transport with fully interactive chemistry in time-dependent calculations and changes in 16 different photolysis rates, whereas Madronich and Granier (1992) inferred changes in the global levels of OH and CH_4 from changes in $J_B(O_3)$ through R1 and R2 by assuming the same trend for OH as they calculated for $J_B(O_3)$. In view of our results, their estimates of changes in OH and CH_4 are thus likely to be overestimates.

Before we focus on changes in the distributions of tropospheric O_3 and OH, it will be useful to present the calculated fields for these gases. Figure 4 shows the calculated mixing ratios of O_3 at noon for April as function of latitude and altitude, while Figure 5 shows the diurnally averaged OH concentrations for May. Both figures show calculated fields for 1990 with J-values representing 1970 conditions (case A). In other words, the figures show how the O_3 and OH distributions for this year might have been if the UV fluxes did not change from the 1970 levels. The calculated O_3 distribution reproduces the general pattern in the observed O_3 distribution from London and Liu (1992). The OH distribution for May is characterized by large gradients, with the highest concentrations located in the lower free troposphere at low Northern latitudes.

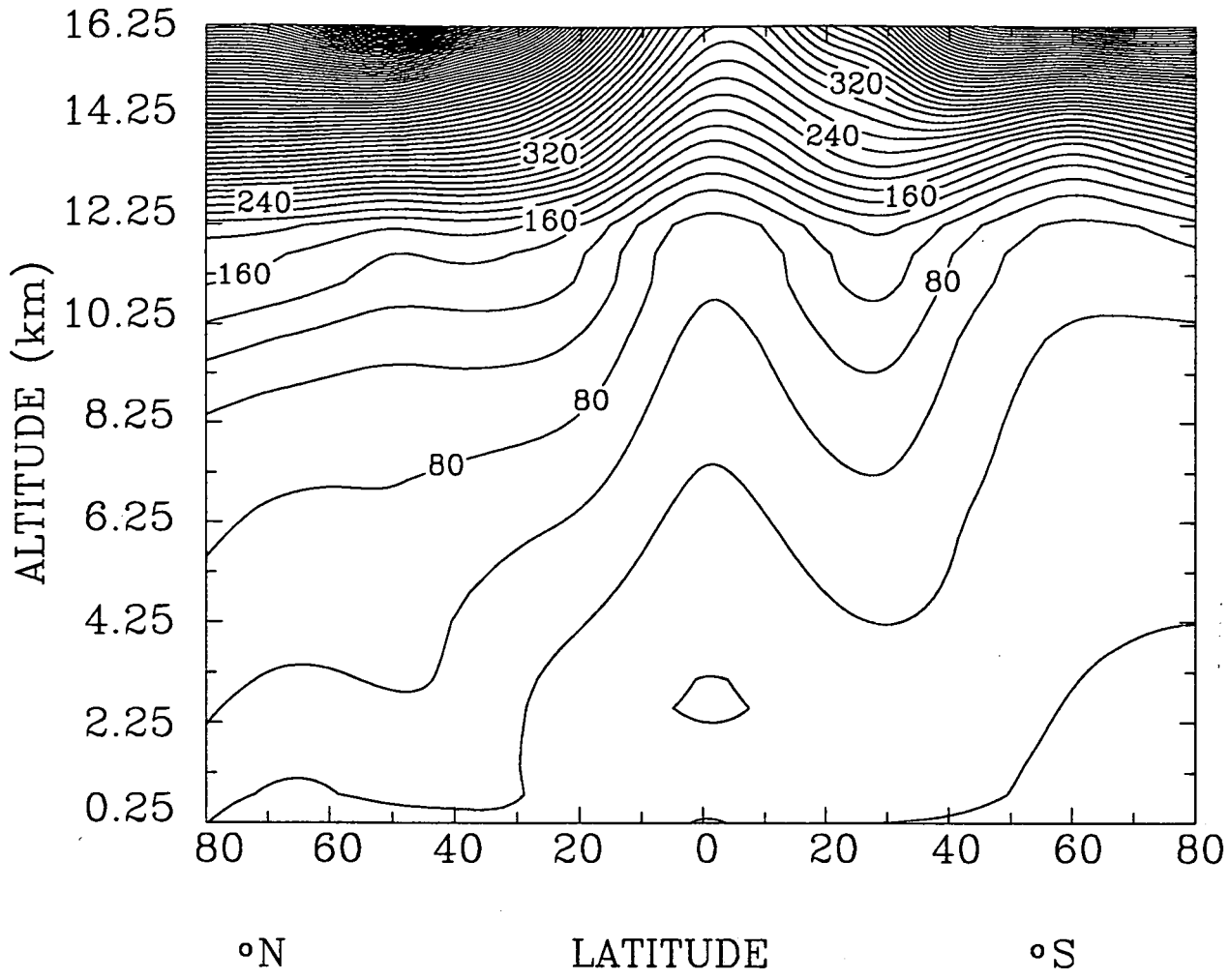

Figure 4. Calculated noon values of O_3 in ppbv for April as function of latitude and altitude for 1990 with J-values representing 1970 conditions (case A).

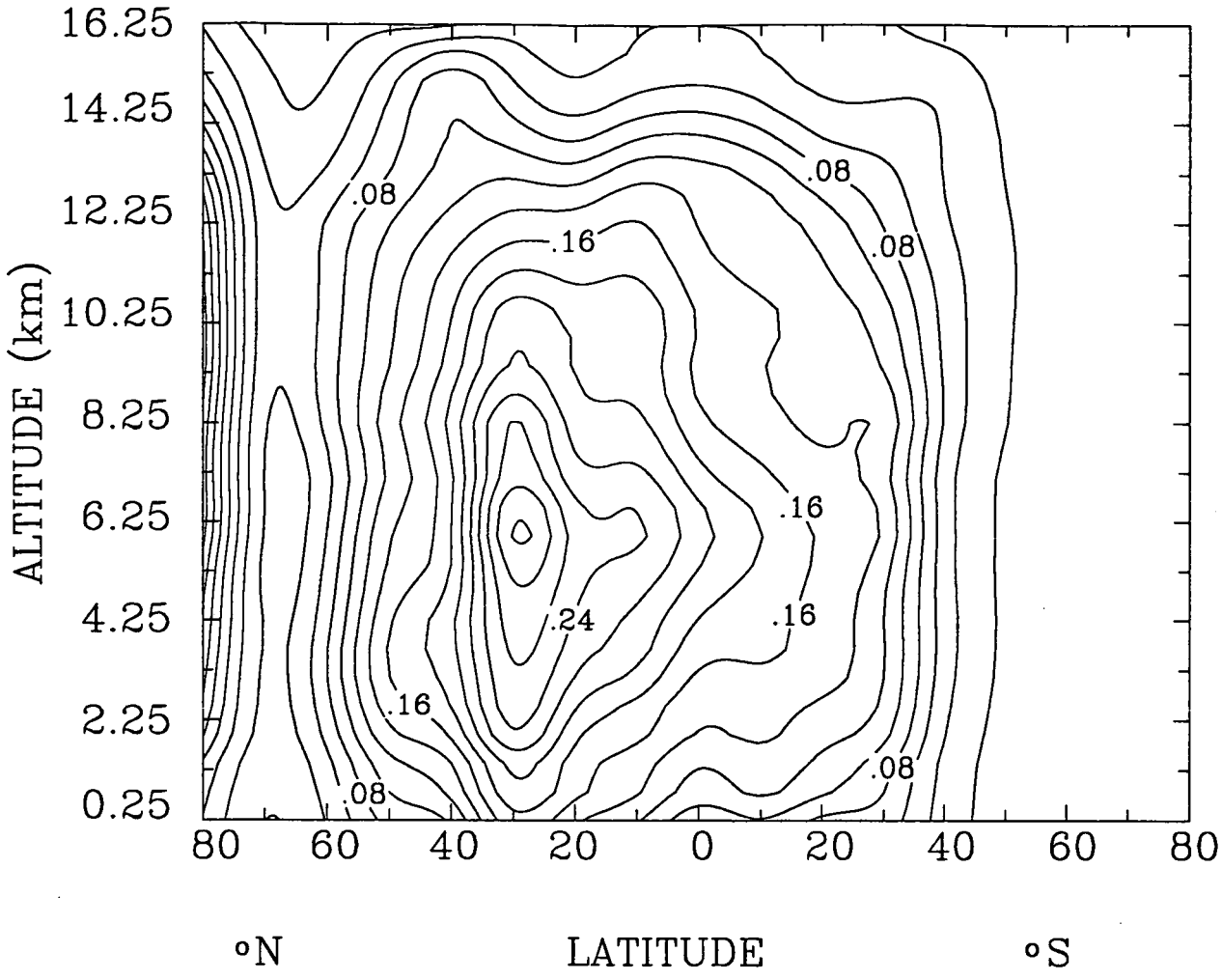

Figure 5. Diurnally averaged OH concentrations for May as function of altitude and latitude (10^7 molecules/cm^3) for 1990 with J-values representing 1970 conditions (case A).

O_3, OH and H_2O_2 are significant species in several processes and the marked changes in these gases may therefore affect other important properties of the atmosphere. We will therefore look more closely at these species. While Figure 3 shows the development in the global annual average levels, it may be of interest to consider

their intra-annual and spatial responses to changes in UV radiation. The effects of changes in UV radiation may be seen in Figure 6a-f which show the percentage difference for 1990 between case B and A in the levels of O_3, OH and H_2O_2 as functions of altitude and latitude for some selected months. In April (Figure 6a), there are increases in tropospheric ozone north of 40°N, while there are reductions elsewhere. The increase in ozone at high Northern latitudes is limited in time, and in June ozone is reduced at all latitudes. The reductions reach 10 % at high Northern latitudes. In December (Figure 6b), the reductions reach 12 % south of 70°S while the reductions are small in the Northern Hemisphere. The maximum reductions in tropospheric O_3 in the unpolluted Southern Hemisphere occur 2 months after the maximum reductions in stratospheric ozone. This is not the case at high Northern latitudes where the maximum reductions in stratospheric ozone take place in March. The tropospheric levels of ozone increase in response to the stratospheric reductions, and in April the increases reach maximum levels. In the following months the sign of the response in tropospheric ozone change, and the reductions in tropospheric ozone are largest in June. This difference between the hemispheres can be explained by the different levels of ozone precursors, especially NOx. Ozone precursors accumulate during winter, and when the UV radiation increases in spring, the chemical activity increases strongly, thereby significantly affecting the ozone chemistry leading to net ozone production for a period.

The reductions in tropospheric O_3 is a result of the increased levels of HO_2 which increase the loss rate of O_3 through R6. In regions with high concentrations of water vapour, the loss of ozone through R1 and R2 will also contribute to reduced ozone levels if the NO levels are low. The increases in O_3 taking place at high Northern latitudes in spring may be explained by the high NO levels and thus increased rate of the reaction between HO_2 and NO which leads to O_3 production.

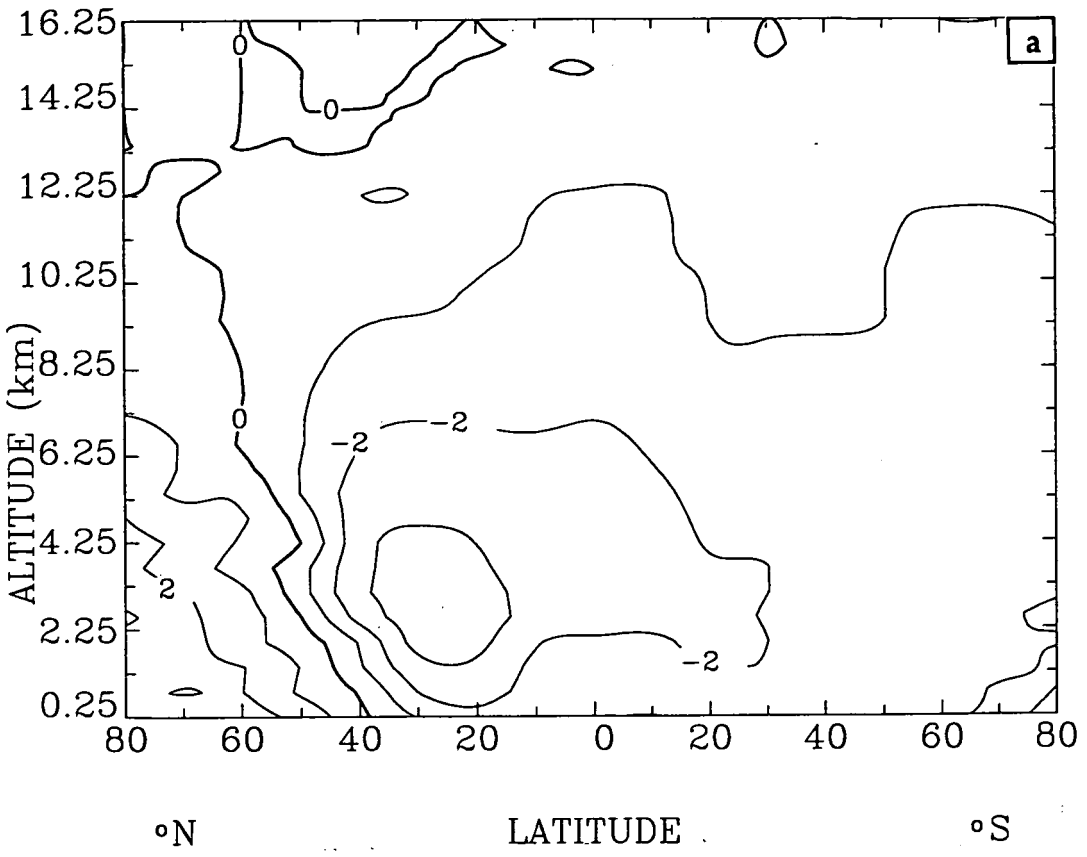
a
16.25
14.25
12.25
10.25
8.25
6.25
4.25
2.25
0.25
ALTITUDE (km)
0
0
0
-2
-2
2
-2
80
60
40
20
0
20
40
60
80
°N
LATITUDE
°S

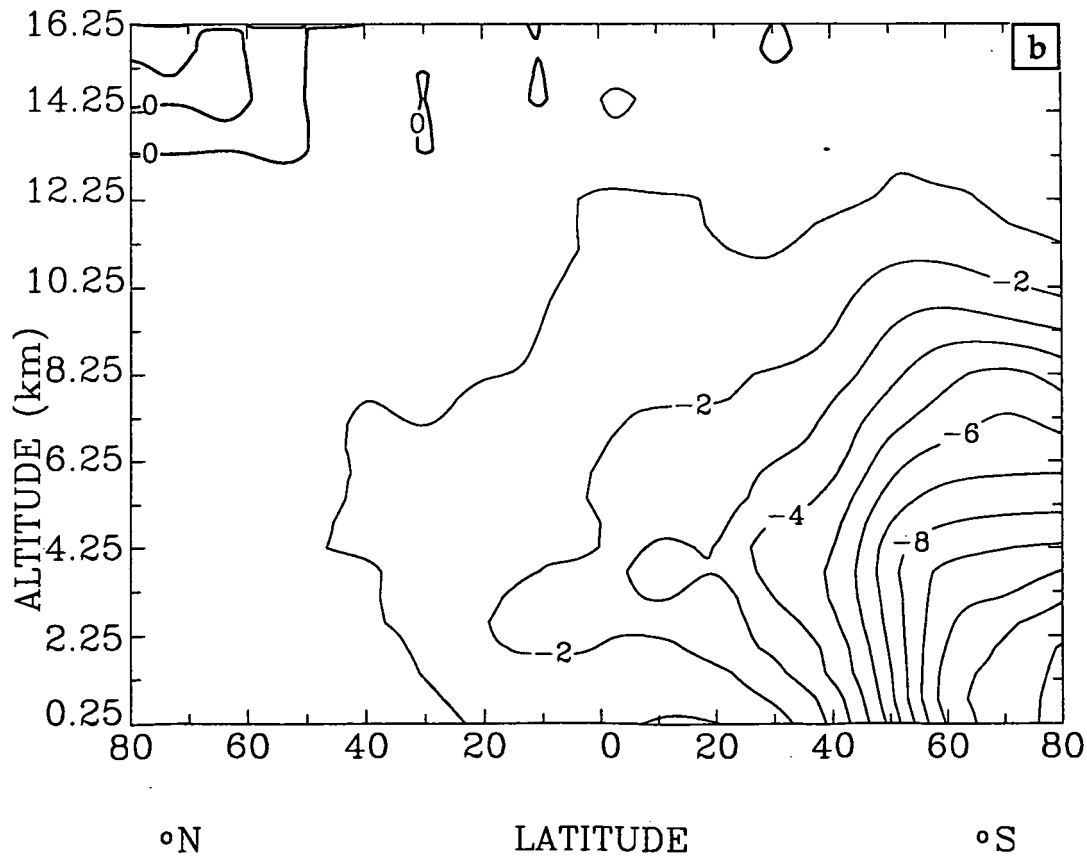
b
16.25
14.25
12.25
10.25
8.25
6.25
4.25
2.25
0.25
ALTITUDE (km)
0
0
0
-2
-2
-6
-4
-8
-2
80
60
40
20
0
20
40
60
80
°N
LATITUDE
°S

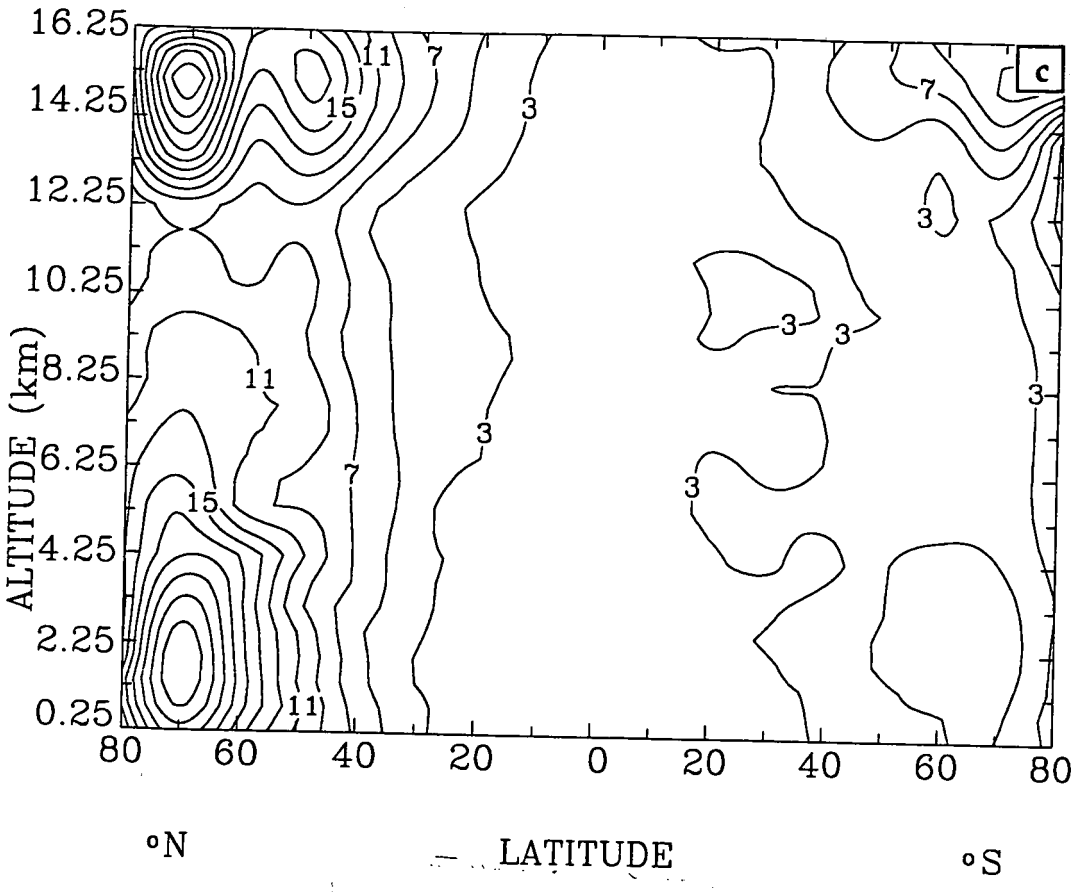
c
16.25
14.25
12.25
10.25
8.25
6.25
4.25
2.25
0.25
ALTITUDE (km)
80 60 40 20 0 20 40 60 80
°N
LATITUDE
°S

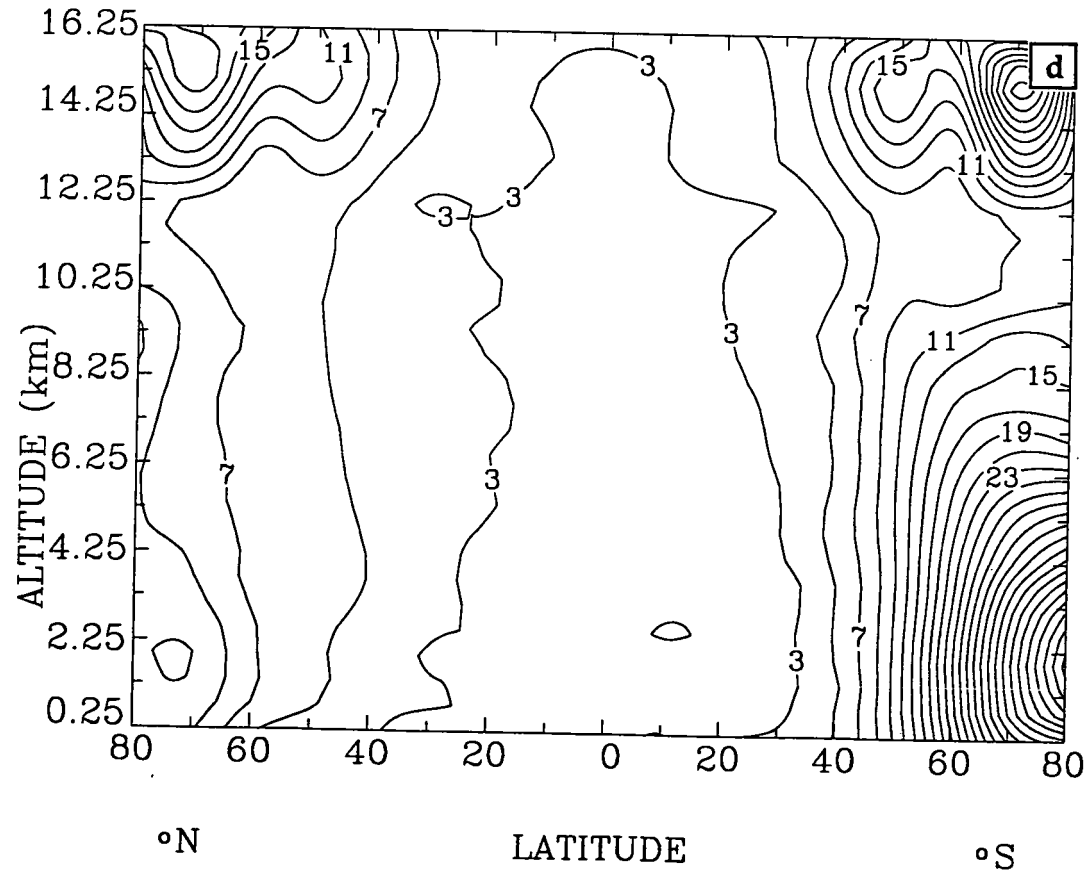
d
16.25
14.25
12.25
10.25
8.25
6.25
4.25
2.25
0.25
ALTITUDE (km)
80 60 40 20 0 20 40 60 80
°N
LATITUDE
°S

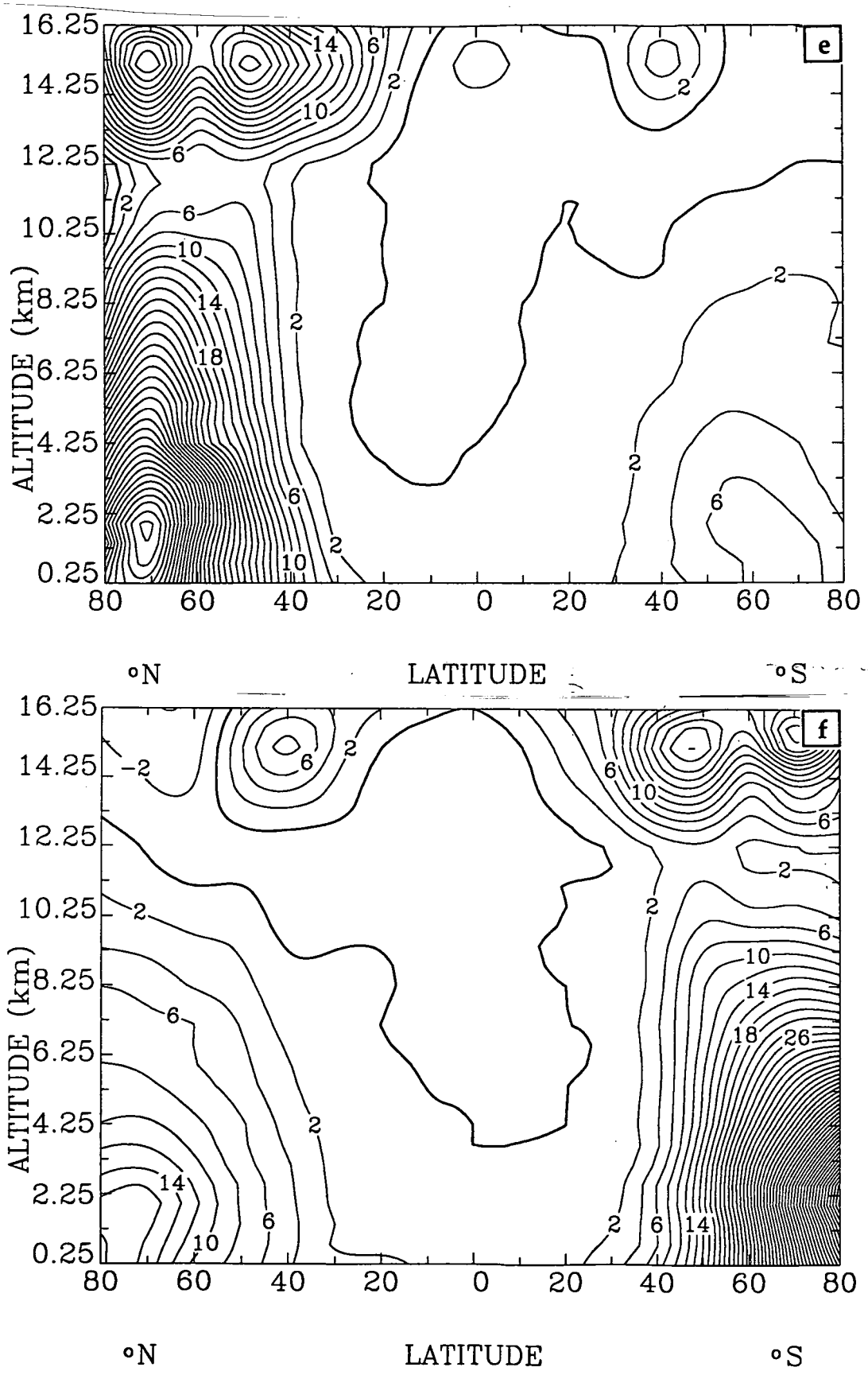

Figure 6. Percentage changes between case B and A for 1990 conditions in a) O_3, April, b) O_3, December, c) OH, May, d) OH, October, e) H_2O_2, May, f) H_2O_2, October.

The results for high Southern latitudes may be compared to observations by Schnell et al. (1991). They found a 17 % reduction in surface ozone at the South Pole in December, January and February over the period 1976-1990. Several explanations are possible, but Schnell et al. (1991) point to the increased photochemical destruction of O_3 from increased UV penetration as a main mechanism.

The increases in OH in May (Figure 6c) reach ~27 % at high Northern latitudes, while there are minor changes south of 30°N. In October (Figure 6d), OH increase by up to ~50 % at high Southern latitudes, with moderate increases elsewhere. The levels of H_2O_2 increase by up to ~70 % at high Northern latitudes in May (Figure 6e). In October (Figure 6f), the H_2O_2 levels increase by more than 70 % over high Southern latitudes, while there are significant changes also over high Northern latitudes. In both months there are slight reductions (< 2%) in the middle troposphere at lower latitudes and in the upper troposphere.

The 1990 responses in tropospheric ozone are moderate, for OH they are moderate to large, while for H_2O_2 the changes are rather large. The calculated net increase in H_2O_2 can be explained by the quadratic relation to HO_2 (reaction R8). In most regions this increase in production dominates over the increased loss through photolysis and the reaction with OH. There is also large spatial variability in the changes in O_3, OH and H_2O_2.

The latitudinal and temporal distribution of ozone column densities in 2050 is different from the 1970 distribution, with decreases at high latitudes in late winter and early spring, and slight increases at low latitudes. One may therefore expect redistributions of the tropospheric components that we have focused on. The levels of tropospheric ozone have increases slightly in the lower and middle troposphere at low and middle latitudes, depending on the time of year. Small reductions are seen at high Northern latitudes in June. The levels of OH and H_2O_2 still show increases at higher latitudes in late winter/early spring, and at low latitudes there are small decreases (see chapter 5 for description of the changes in total ozone in 2050).

7. The significance of UV increases for other environmentally important atmospheric constituents

In addition to reducing the concentration of greenhouse gases like O_3 and CH_4, increases in OH will also reduce the concentration of several other gases (CO, NMHC, sulphur containing gases, etc.) and also greenhouse gases like HCFCs (hydrochlorofluorocarbons) and HFCs (hydroflourocarbons). For gases with relative short chemical lifetimes (days to a few months), the spatial distributions may also be affected. As an example we might expect variation in the spatial NOx chemistry since increased OH levels will increase the transfer of NO_2 to HNO_3. This is the main loss mechanism for NOx, and increased OH may therefore reduce the dispersion of NOx on regional scales and thereby limit the spatial extension of ozone formation.

Oxidation of SO_2 to sulphate particles may also be changed, either through gas phase oxidation (by OH) or through liquid phase oxidation (by H_2O_2 and O_3). This is of significance for climate since increased concentrations of such particles may affect the Earth's radiative balance by backscattering of solar radiation (IPCC, 1992). Increases in the transfer of SO_2 to sulphate may also allow larger fractions of the sulphur emitted to be transported over longer distances since the lifetime of sulphate is larger than the lifetime of SO_2. Increased transfer of SO_2 to sulphate may therefore affect the regional distribution of acid deposition.

Reductions in tropospheric O_3 and CH_4 reduce the radiative forcing of climate. Since there are evidences that ozone depletion can be connected to increased levels of CFC released chlorine in the stratosphere, the reductions in tropospheric O_3 and CH_4, due to the reductions in stratospheric ozone, therefore represent a damping effect on the global warming from CFCs. Calculations of the change in radiative forcing should be performed to assess the climatic implications of these effects.

8. Other factors controlling tropospheric O_3 and OH

Numerous studies have addressed how changes in emissions may affect the tropospheric levels of gases as O_3 and OH (Isaksen, 1980; Thompson and Cicerone, 1986; Isaksen and Hov, 1987; Thompson et al., 1989; Thompson et al., 1990; Crutzen and Zimmermann, 1992; Isaksen et al., 1992).

The levels of NO control the responses in O_3 and OH to increased emissions of CO and hydrocarbons (Crutzen, 1987). Increased emissions of NOx generally increase the levels of O_3. However, during winter at high latitudes or in highly polluted areas, increased emissions of NOx may reduce the levels of ozone. Increased emissions of NOx generally increase the levels of OH through a redistribution through R5 and through increased O_3 levels. In some situations, increased emissions of NOx may also significantly reduce the OH levels through increased OH loss via R11.

Increased emissions of CO and CH_4 increase the O_3 levels, while they generally reduce the OH levels. Due to the longer lifetime of CH_4 (~10 years) than of CO (2-3 months), the former may affect the chemistry on larger spatial scales.

Changes in tropospheric concentrations of water vapour may occur as a consequence of climate change. Through R2 such changes will affect the production of OH. As in the case of increased OH production through UV-B increases, the response in the concentrations of OH to increased water vapour densities will be less than the initial increase in production, due to the quadratic relationship between OH concentration and production. Changes in water vapour may, through the effects on the levels of HOx, further affect O_3 and CH_4.

9. Limitations and uncertainties

In this study several possible indirect effects and feedbacks have not been included due to the nature of the approach that has been applied. We have used separate models for the stratosphere, the J-value calculations and for the troposphere and these models are not linked in an interactive way. Any feedbacks between the troposphere and the stratosphere are therefore not taken into account. The models of the stratosphere and the troposphere have fixed transport thus excluding possible dynamical effects due to changes in the concentrations of gases that affect the radiative fluxes. Changes in the oxidizing capacity of the troposphere may also change the flux to the stratosphere of ozone controlling gases like HCFCs and CH_4. This could constitute a feedback loop since the resulting changes in stratospheric O_3 further could affect tropospheric chemistry through UV changes.

Although the dissociation rates are sensitive to cloud occurrence and cloud properties we consider the accuracy in the calculation of dissociation rates as good. Depending on cloud albedo, cloud reflection may result in a preferential enhancement of NO_2 photolysis compared to O_3, resulting in enhanced O_3 production above clouds (Thompson, 1984). Madronich (1987) found that within the clouds the actinic flux may increase by as much as a factor of 5 in the upper part of a cloud compared to clear sky conditions. The actinic flux was shown to be particularly sensitive to the optical thickness of the cloud. Similar results have been obtained with our model (Jonson and Isaksen, 1991; Jonson and Isaksen, 1993; this work). As a consequence of the high sensitivity of the dissociation rates to cloud occurrence, extension and optical properties, it appears that the interpretation of the tropospheric model results is sensitive to the cloud representation. Unfortunately, observations of clouds and cloud properties are scarce. However, as we are primarily interested in calculated changes rather than the actual concentrations, much of the uncertainties related to clouds are likely to cancel out.

The two-dimensional approach for studies of tropospheric chemistry is likely to be connected with uncertainties. NOx is a key component for tropospheric O_3 and OH.

There are large zonal variations in the emission intensity of NOx and thereby also in the atmospheric concentrations since the lifetime of NOx is only a few days, while the zonal transport time is approximately 2 weeks. By assuming zonal homogeneity, the ability to model some important non-linear effects in tropospheric chemistry is reduced. Kanakidou and Crutzen (1992) studied the effects of zonal averaging. They used a global three-dimensional (3D) chemistry/transport model and assumed longitudinally uniform emissions of NOx and NMHC (2D mode) and compared the results obtained with results from the same 3D model, but now with longitudinally varying emissions. They found that in 2D mode the model overestimated the middle and the low tropospheric levels of O_3 and OH in the tropics and middle Northern latitudes compared to the 3D case. Their study also gave an overestimation in the amount of methane oxidized by approximately 20% in the 2D case relative to the 3D case.

In earlier studies the effects of changed NOx emissions on ozone are found to be quite sensitive to the background levels of NOx (Isaksen et al., 1992). Several processes affect the levels of NOx in the background troposphere. Important among these are convective transport from the boundary layer, production of NOx from lightning, input from the stratosphere and decomposition of PAN. To get some impression of the sensitivity of the results to the background concentrations of NOx, the steady state runs for 1970 and 1990 were performed with a NOx production from lightning of 2 TgN/yr and 20 TgN/yr. The assumptions about this source strength has significant effects on the emission of methane necessary to sustain an atmospheric mixing ration of 1.7 ppmv, as well as for the calculated global averages of O_3 and OH. But the modelled relative changes in O_3, OH and CH_4 between the 1970 and 1990 runs are negligible. In addition, the spatial pattern of the changes in O_3 and OH are quite similar. Thus, it may be concluded that the assumed emissions of NOx and modelled background levels of this gas are not of critical importance for the conclusions in our study on changes in trace gas distributions.

Recent progress in atmospheric chemistry has underlined the importance of including heterogeneous chemistry in the models. In the stratospheric chemistry model,

heterogeneous chemistry between the gas phase and PSCs and background particles is included. In the tropospheric model only gas phase chemistry is modelled. First order scavenging of soluble species by clouds, rain and aerosols are, however, included. Tropospheric chemistry models that include aqueous phase chemistry and exchange processes between the gaseous and the aqueous phase, give lower levels of ozone (Lelieveld and Crutzen, 1990; Lelieveld and Crutzen, 1991; Jonson and Isaksen, 1993; Jonson and Isaksen, 1994). Jonson and Isaksen (1994) report up to ~20 % lower levels in ozone when heterogeneous chemistry is included, with the largest reductions taking place in the remote middle troposphere. The omission of heterogeneous chemistry in the troposphere in our study may constitute only a small error since we are focusing on changes in the levels of the gases.

10. Conclusions

In this study it is shown that reductions in stratospheric O_3, and the subsequent increase in the fluxes of UV-B into the troposphere, lead to large increases in the photolysis rate of O_3 ($J_B(O_3)$) that initiates OH production. The relative increase in the photolysis rate is larger than the relative decrease in stratospheric ozone. The amplification of $J_B(O_3)$ is, however, counteracted by damping mechanisms in the chemistry of the troposphere. This underlines the importance of including a fully interactive chemistry in such studies. All the three most important oxidizing species (OH, O_3 and H_2O_2) are affected. The levels of OH and H_2O_2 increase, while the levels of tropospheric O_3 are generally reduced. However, in a limited region, there are increases in tropospheric O_3 in response to increased UV, which are due to the role of NO. The magnitude of the changes vary considerably with region and time of year. Through increases in OH, the global level of CH_4 is reduced. Because of its long lifetime, the maximum effect on methane is delayed by approximately 10 years. For 2050, our calculations give a global level of total ozone that is approximately equal to the 1970 level. But the latitudinal distribution is somewhat altered, and thus slight redistributions of tropospheric O_3, OH and H_2O_2 are derived for 2050. Due to the radiative properties of tropospheric O_3 and CH_4, reduced levels of these gases will

reduce the radiative forcing of climate. This mechanism constitute a negative indirect chemical effect on climate from the ozone depleting substances, mainly CFCs. In this paper we have chosen to study the impact of increased UV from reductions in stratospheric ozone alone on the levels of OH. How changes in water vapour densities or emissions of various gases affect the chemistry of OH have not been considered here. For instance, reduced emissions of methane itself may, of course, also explain the reduced growth rate in the atmospheric concentrations. Nevertheless, it is shown that the reductions in stratospheric O_3, and the subsequent increase in the fluxes of UV into the troposphere, may have contributed to the observed reduction in the growth rate for methane.

Acknowledgements

One of us (J.E.J.) has been supported by NAVF (Norwegian Research Council for Science and Humanities) under grant 447.90/016b. We thank Elena Abilova for programming assistance, Terje Berntsen for valuable discussions and programming assistance and Bjørg Rognerud for help in conducting calculations of ozone column densities.

Table 1 Chemical reaction scheme applied in the model. The number in the cloumn labeled ref. refers to the reference for the raction rates. 1 is Watson et al. (1990), 2 is Atkinson et al. (1989), 3 is Atkinson (1990), 4 is Vaghjiani and Ravishankara (1989), 5 is Vaghjiani and Ravishankara (1991), 6 is DeMore et al. (1992), 7 is Atkinson et al. (1992), 8 is Madronich and Calvert (1990).

Model ref.	Reactions	Rate constants A	Rate constants -E_a/R	Ref.	Note
C2MA	$O(^1D) + M(O_2) \rightarrow O(^3P) + M$	3.2E-11	70	1	
C2MA	$O(^1D) + M(N_2) \rightarrow O(^3P) + M$	1.8E-11	110	1	
C2M = C2MA*0.21 + C2MB*0.79					
C222	$O(^1D) + H_2O \rightarrow 2OH$	2.2E-10		1	
C104M	$O(^3P) + O_2 + M \rightarrow O_3 + M$		Tab. 2	6	
C110	$O(^3P) + NO_2 \rightarrow NO + O_2$	6.5E-12	120	1	
C709	$O_3 + NO \rightarrow NO_2 + O_2$	2.0E-12	-1400	1	
C710	$O_3 + NO_2 \rightarrow NO_3 + O_2$	1.2E-13	-2450	1	
C719	$O_3 + OH \rightarrow O_2 + HO_2$	1.6E-12	-940	1	
C720	$O_3 + HO_2 \rightarrow OH + 2O_2$	1.1E-14	-500	1	
C2020A	$HO_2 + HO_2 \rightarrow H_2O_2 + O_2$	2.3E-13	600	1	
C2020B	$HO_2 + HO_2 + M \rightarrow H_2O_2 + O_2 + M$	1.7E-33[M]	1000	1	
C2020 = C2020A + C2020B					
C1923	$OH + H_2O_2 \rightarrow H_2O + HO_2$	2.9E-12	-160	1	
C1019X	$OH + NO_2 + M \rightarrow HNO_3 + M$		Tab. 2	6	
C920	$NO + HO_2 \rightarrow NO_2 + OH$	3.7E-12	240	1	
C1011	$NO_2 + NO_3 \rightarrow NO + NO_2 + O_2$	2.5E-14	-1230	6	
C1011M	$NO_2 + NO_3 + M \rightarrow N_2O_5 + M$		Tab. 2	6	4
C14M	$N_2O_5 + M \rightarrow NO_2 + NO_3 + M$			1	4
C1020	$NO_2 + HO_2 + M \rightarrow HO_2NO_2 + M$		Tab. 2	6	5
CHO2NO2	$HO_2NO_2 + M \rightarrow HO_2 + NO_2 + M$			1	5

model ref.	Reactions	Rate constants A	Rate constants -E_a/R	Ref.	Note
C911	$NO + NO_3 \rightarrow 2NO_2$	1.7E-11	150	1	
C1920	$OH + HO_2 \rightarrow H_2O + O_2$	4.8E-11	250	1	
C1926	$OH + HNO_3 \rightarrow NO_3 + H_2O$			1	1
C1929X	$OH + HO_2NO_2 \rightarrow NO_2 + O_2 + HO_2$	1.3E-12	380	1	
C1945	$OH + CO + O_2 \rightarrow HO_2 + CO_2$			1	2
C1956	$OH + CH_4 \rightarrow CH_3 + H_2O$			5	3
C1957	$OH + C_2H_4 \rightarrow CH_3 + CH_2O$		Tab. 2	6	
C757	$O_3 + C_2H_4 \rightarrow HCHO + 0.12HO_2 + 0.44CO$	1.2E-14	-2630	1	
C1959X	$OH + C_2H_6 \rightarrow C_2H_5O_2 + H_2O$	1.1E-11	-1100	1	
C1959	$OH + C_3H_6 \rightarrow CH_3XX$	4.85E-12	504	2	
C759	$O_3 + C_3H_6 \rightarrow 0.25HO_2 + 0.5(CH_2O + CH_3CHO) + 0.15OH + 0.03CH_3O + 0.31CH_3 + 0.07CH_4 + 0.4CO$	6.5E-15	-1900	1	
C1960	$OH + C_4H_{10} \rightarrow C_4H_9O_2 + H_2O$			1	6
C1962	$OH + C_6H_{14} \rightarrow C_6H_{13}O_2 + H_2O$	5.61E-12		3	
C1959C	$OH + C_6HXR \rightarrow$ 0.6*AR1	1.04E-11		3	
C1965	$OH + ISOPRENE \rightarrow AR4$	2.54E-11	410	3	13
C449M	$CH_3 + O_2 + M \rightarrow CH_3O_2 + M$		Tab. 2	6	
C5151A	$CH_3O_2 + CH_3O_2 \rightarrow 0.4 * (2CH_3O + O_2)$	2.2E-13	220	1	
C5151B	$\rightarrow 0.6 * CH_2O$			1	
C450	$CH_3O + O_2 \rightarrow HO_2 + CH_2O$	3.9E-14	-900	1	
C1948	$OH + CH_2O \rightarrow CHO + H_2O$	1.0E-11	0	1	
C447	$CHO + O_2 \rightarrow HO_2 + CO$	3.5E-12	140	1	

Model ref.	Reactions	Rate constants A	-E_a/R	Ref.	Note
C2051	$CH_3O_2 + HO_2 \rightarrow CH_3O_2H + O_2$	3.3E-13	800	1	
C1956A	$OH + CH_3O_2H \rightarrow CH_3O_2 + H_2O$	1.79E-12	219	4	
C1956B	$OH + CH_3O_2H \rightarrow CH_2O + OH + H_2O$			4	7
C19AR2	$OH + AR2 \rightarrow AR3$	2.0E-11		0	
C19AR5	$OH + AR5 \rightarrow AR6$	2.0E-11		0	13
C1980	$OH + CH_3COX \rightarrow CH_3COB$				15
C1964A1	$OH + HCOHCO \rightarrow fa * (CHO + CO)$	1.1E-11		2	14
C1964A2	$\rightarrow fb * (CH_3CO)$				14
C1964A3	$\rightarrow fc * (2CO + HO_2)$				14
C1964B	$OH + RCOHCO \rightarrow CH_3CO + CO$	1.7E-11		3	15
C951C	$NO + CH_3O_2 \rightarrow fa * (NO_2 + CH_3O)$	4.2E-12	180	1	8
C960G	$NO + C_2H_5O_2 \rightarrow fa * (NO_2 + (1 - fb) * (CH_2O + CH_3) + fb * (HO_2 + CH_3CHO))$	4.9E-12	180	1*	8,9
C960C	$NO + C_4H_9O_2 \rightarrow fa * (NO_2 + (1 - fb(CH_3CHO + C_2H_5O_2) + fb * (HO_2 + CH_3COX))$	4.9E-12	180	1*	
C962C	$NO + C_6H_{13}O_2 \rightarrow fa * (NO_2 + C_4H_9O_2 + CH_3CHO)$	4.9E-12	180	1*	10
C9AR1	$NO + AR1 \rightarrow NO_2 + HO_2 + AR2 + RCOHCO$	4.2E-12	180	1**	
C9AR3	$NO + AR3 \rightarrow NO_2 + HO_2 + HCOHCO + RCOHCO$	4.2E-12	180	1**	
C9AR4	$NO + AR4 \rightarrow fa(NO_2 + HO_2 + AR5 + CH_2O)$	4.2E-12	180	1**	13
C9AR6	$1.5NO + AR6 \rightarrow 1.5NO_2 + 0.67HO_2 + 0.43CH_2O + 0.67RCOHCO + 0.33CH_3CO + 0.33CH_3CHO$	4.2E-12	180	1**	13
C960J	$NO + CH_3COB \rightarrow f * (NO_2 + HO_2 + CH_3COY)$	4.2E-12	180	1**	8
C972	$NO + CH_3XX \rightarrow NO_2 + CH_2O + CH_3CHO + HO_2$	4.2E-12	180	1**	
C1973	$OH + CH_3CHO \rightarrow CH_3CO + H_2O$	6.0E-12	250	1	

* Rate assumed to be 1.16 times faster than C951C, as Atkinson et al. (1989), give k_{298} 1.16 times faster for $C_2H_5O_2 + NO$ than for $CH_3O_2 + NO$.

** Rate assumed to be equal to C951C ($NO + CH_3O_2$)

Model ref.	Reactions	Rate constants A	Rate constants $-E_a/R$	Ref.	Note
C474	$CH_3CO + O_2 \rightarrow CH_3COO_2$	5.0E-12		2	
C975	$CH_3COO_2 + NO \rightarrow CH_3 + NO_2 + CO_2$	1.4E-11		2	
C1075	$CH_3COO_2 + NO_2 + M \rightarrow PAN + M$		Tab. 2	6	
C76	$PAN + M \rightarrow CH_3COO_2 + NO_2 + M$		Tab. 2	7	
C1959S	$OH + PAN \rightarrow CH_2O + NO_2 + CO_2 + H_2O$	1.2E-12	-650	2	
C5175A	$CH_3COO_2 + CH_3O_2 \rightarrow CH_3O + CH_3 + CO_2 + O_2$	5.5E-12		2	
C5175B	$CH_3COO_2 + CH_3O_2 \rightarrow CH_2O + CH_3COOH + O_2$	5.5E-12		2	
C5160G	$CH_3O_2 + C_2H_5O_2 \rightarrow 0.5(CH_3O+ (1-f)(CH_2O + CH_3) f(HO_2 + CH_3CHO)) +0.25(CH_2O + CH_3CHO)$	1.0E-13		3,8	16
C5160C	$CH_3O_2 + C_4H_9O_2 \rightarrow 0.5(CH_3O+ (1-f)(CH_3CHO + C_2H_5O_2) f(HO_2 + CH_3COX)) +0.25(CH_2O + CH_3COX)$	1.0E-13		3,8	16
C5162C	$CH_3O_2 + C_6H_{13}O_2 \rightarrow CH_3O + CH_3CHO+ C_4H_9O_2$	1.0E-13		3	
C5172	$CH_3O_2 + CH_3XX \rightarrow CH_3O + CH_3CHO+ CH_2O + HO_2$	1.0E-13		3	
C5160J	$CH_3O_2 + CH_3COB \rightarrow CH_3O + HO_2 + CH_3COY$	1.0E-13		3	
C51AR4	$CH_3O_2 + AR4 \rightarrow CH_2O + CH_3O + HO_2 + AR5$	1.0E-13		3	
C51AR6	$CH_3O_2 + AR6 \rightarrow RCOHCO + CH_3O + HO_2$	1.0E-13		3	
CARAD	$HO_2 + ARAD \rightarrow CH_3O_2H$	6.5E-13	650	2	11
C1928	$SO_2 + OH \rightarrow SO_4$	1.2E-12			
C2028	$SO_2 + HO_2 \rightarrow SO_4 + OH$	1.0E-18		1	
C2851	$SO_2 + CH_3O_2 \rightarrow SO_4$	1.0E-17		1	

Table 2

Reaction	Rate constants k_0	k_{inf}	F_c
C104M	$6.0E\text{-}34(T/300)^{-2.3}[M]$		
C449M	$4.5E\text{-}31(T/300)^{-3.0}[M]$	$1.8E\text{-}12(T/300)^{-1.7}$	0.6
C1019X	$2.6E\text{-}30(T/300)^{-3.2}[M]$	$2.4E\text{-}11(T/300)^{-1.3}$	0.6
C1011M	$2.2E\text{-}30(T/300)^{-3.9}[M]$	$1.5E\text{-}12(T/300)^{-0.7}$	0.6
C1020	$1.8E\text{-}31(T/300)^{-3.2}[M]$	$4.7E\text{-}12(T/300)^{-1.4}$	0.6
C1957	$1.0E\text{-}28(T/300)^{-0.8}[M]$	8.8E-12	0.6
C1075	$8.0E\text{-}29(T/300)^{-7.0}[M]$	$1.2E\text{-}11(T/300)^{-1.0}$	0.6
C76	$4.9E\text{-}3e^{(-12100/T)}[N_2]$	$4.0E+16e^{(-13600/T)}$	0.3

Table 3 Photolytic reactions

Model ref.	Reactions
DAO3	$O_3 + h\nu \rightarrow O(^3P) + (O_2)$
DBO3	$O_3 + h\nu \rightarrow O(^1D) + (O_2)$
DNO2	$NO_2 + h\nu \rightarrow NO + O(^3P)$
DH2O2	$H_2O_2 + h\nu \rightarrow 2OH$
DHNO3	$HNO_3 + h\nu \rightarrow NO_2 + OH$
DACH2O	$HCHO + h\nu \rightarrow CHO + HO_2$
DBCH2O	$HCHO + h\nu \rightarrow CO + (H_2)$
DCH3CHO	$CH_3CHO + h\nu \rightarrow CHO + CH_3$
DCH3COX	$CH_3COCH_2CH_3 + h\nu \rightarrow CH_3CO + C_2H_5O_2$
DCH3COY	$CH_3COCOCH_3 + h\nu \rightarrow 2CH_3CO$
DHCOHCO	$HCOCHO + h\nu \rightarrow CO + HCHO$
DRCOHCO	$CH_3COCHO + h\nu \rightarrow CO + CH_3CHO$
DNO3	$NO_3 + h\nu \rightarrow NO_2 + O(^3P)$
DN2O5	$NO_2NO_3 + h\nu \rightarrow NO_2 + NO_3$
DCH3O2H	$CH_3O_2H + h\nu \rightarrow OH + CH_3O$
DHO2NO2	$HO_2NO_2 + h\nu \rightarrow NO_2 + HO_2$

Note 1 : $k = k_0 + k_3[M]/(1 + k_3[M]/k_2)$
where $k_0 = 7.2 \times 10^{-15} e^{(785/T)}$, $k_2 = 4.1 \times 10^{-16} e^{(1440/T)}$ and
$k_3 = 1.9 \times 10^{-33} e^{(725/T)}$

Note 2 : $1.5 \times 10^{-13}(1.0 + 0.6 P_{atm})$
where P_{atm} is air pressure in atmospheres.

Note 3 C1956 : $k = 1.59 * 10^{-20} * T^{2.84} * e^{-984/T}$

Note 4 : Equlibrium const. for $NO_2 + NO_3 \rightarrow N_2O_5$ is
$k_{eq} = 4.0E - 27e^{(10930./T)}$. Reaction rate for $N_2O_5 \rightarrow NO_2 + NO_3$ is then given as C1011M/k_{eq} .

Note 5 : Equlibrium const. for $HO_2 + NO_2 \rightarrow HO_2NO_2$ is
$k_{eq} = 2.1E - 27e^{(10900./T)}$. Reaction rate for $HO_2NO_2 \rightarrow HO_2 + NO_2$ is then given as C1020/k_{eq} .

Note 6 C1960/R4010 : $k = 1.51 * 10^{-17} * T^{2.0} * e^{190/T}$

Note 7 C1956A + C1956B = $2.93E - 12 * e^{190/T}$, C1956B = $2.93E - 12 * e^{190/T}$-C1956A

Note 8 The fraction ($1 - fa, fa = k_b/k_a + k_b$) of organic nitrates ($RONO_2$) formed from the reaction RO_2 + NO $\longrightarrow$ (1-fa)$RONO_2$ +fa(NO_2 + RO) is calculated by the following equations (Atkinson, 1990)

$$\frac{k_a}{k_b} = \left\{ \frac{Y_0^{300}[M](T/300)^{-m_0}}{1 + \frac{Y_0^{300}[M](T/300)^{-m_0}}{Y_\infty^{300}[M](T/300)^{-m_\infty}}} \right\} F^z$$

$$z = \left[1 + \left(log_{10} \frac{Y_0^{300}[M](T/300)^{-m_0}}{Y_\infty^{300}[M](T/300)^{-m_\infty}} \right)^2 \right]^{-1}$$

where $Y_0^{300} = \alpha e^{\beta N}$, where N is the number of C atoms in the peroxy radical, and $\alpha = 1.94 * 10^{-22}$ and $\beta = 0.97$ are constants. $[M]$ is number density of the air, T is temperature and $m_0 = 0$, $m_\infty = 8.1$, $F = 0.411$ and $Y_\infty^{300} = 0.826$.

Note 9 The alkoxy radicals (RO) formed in the reaction between peroxy radical and NO will either react with O_2 or decompose. Values of fb (fb denotes the fraction reacting with O_2) are calculated on the basis of data given in Atkinson (1990).

Note 10 In the case of $C_6H_{13}O$, decomposition is assumed to be the only reaction since a C6 ketone is not included in the scheme.

Note 11 ARAD is the sum of peroxy radicals (ARAD = $CH3XX + C_6H_{13}O_2 + C_4H_9O_2 + C_2H_5O_2 + CH3COB + AR4 + AR6$)

Note 12 List of abbreviations used in the chemical scheme :

CH3XX	$CH_3CH(O_2)CH_2OH$
CH3COB	$CH_3COCH(O_2)CH_3$
CH3COX	$CH_3COCH_2CH_3$
CH3COY	$CH_3COCOCH_3$
AR4	First RO_2 radical from the reaction of isoprene with OH
AR5	The sum of methylvinylketone (MVK) and methacrolein (MACR)
AR6	RO_2 radical formed from MVK + OH or MACR + OH

Note 13 The scheme for isoprene oxidation is based on Lloyd et al. (1983). Since the uncertainties in the emission estimates are so large only oxidation initilized by reaction with OH is included. The scheme based on assumptions I-III is :

$$\text{Isoprene} + \text{OH} \longrightarrow \text{AR4}$$

$$\text{AR4} + \text{NO} \longrightarrow 0.1\ \text{RONO}_2 + 0.9\ (\text{NO}_2 + \text{HO}_2 + \text{HCHO} + \text{AR5}) \qquad \text{I}$$

$$\text{AR5} + \text{OH} \longrightarrow \text{AR6} \qquad \text{II}$$

$$\text{AR6} + 1.5\ \text{NO} \longrightarrow 1.5\ \text{NO}_2 + 0.67\ (\text{HO}_2 + \text{CH}_3\text{COHCO}) + 0.43\ \text{HCHO} + 0.33\ (\text{CH}_3\text{CHO} + \text{CH}_3\text{CO}) \qquad \text{III}$$

I : AR5 consists of equal amounts of MVK and MACR.
II : MVK and MACR have the same chemical lifetime.
III : All RO_2 radicals in AR6 reacts with the same rate with NO.

In Lloyd et al. (1983) 4 different RO_2 radicals are identified from the reaction of AR5 with OH depending on wether MVK or MACR is oxidized, and the mechanism for the oxidation. The fraction yields of the products in the last equation is derived by considering the fraction yields of the 4 RO_2 radicals and their reaction path to the above products. A simplification is made as the $HOCH_2CO$ radical formed from one of the RO_2 radicals formed from MVK, is treated as CH_3CO in the scheme.

Note 14 Product yields of the reaction of OH with glyoxal is given by Atkinson (1990) as

$$k_a/k = fa = \frac{3.5 * 10^{18}}{3.5 * 10^{18} + 2 * [O_2]}$$

$$k_b/k = fb = \frac{[O_2]}{3.5 * 10^{18} + 2 * [O_2]}$$

$$k_c/k = fc = fb$$

Note 15 $k = 3.2 * 10^{-18} * T^2 * e^{414/T}$, Atkinson (1990).

Note 16 Products taken from Madronich and Calvert (1990). The alkoxy radicals which are products of the reaction are treated according to note 9.

Deposition velocities (cm s^{-1}) for different surface categories.

Species	Land	Sea	Ice/Snow
O_3	0.5	0.1	0.05
HNO_3	1.0	1.0	0.05
CO	0.03	-	-
NO_2	0.2	0.05	0.04
PAN	0.2	0.04	-
H_2O_2	1.0	1.0	0.1

The numbers are based on Crutzen and Zimmerman (1991), Hough (1991) and Müller (1992), and references therein.

References

Atkinson, R. 1990. Gas-phase tropospheric chemistry of organic compounds: A review. *Atmos. Environ., 24A,* No. 1, 1990, 1-44.

Atkinson, R., Baulch, D.L., Cox, R.A., Hampson, R.F., Kerr, J.A. and Troe, J. 1989. Evaluated kinetic and photochemical data for atmospheric chemistry: Supplement III. IUPAC subcommittee on gas kinetic data evaluation for atmospheric chemistry, *J. Phys. Chem. Ref. Data, 18,* 881-1097.

Atkinson, R., Baulch, D.L., Cox, R.A., Hampson, R.F., Kerr, J.A. and Troe, J. 1992. Evaluated kinetic and photochemical data for atmospheric chemistry: Supplement IV. IUPAC subcommittee on gas kinetic data evaluation for atmospheric chemistry, *Atmos. Environ., 26A,* 1197-1230.

Berntsen, T., Solberg, S. and Isaksen, I.S.A. 1989. Calculated changes in the tropospheric distribution of long-lived primary trace species and in secondary species resulting from releases of pollutants. *Report No. 74,* Institute for Geophysics, University of Oslo.

Berntsen, T., Fuglestvedt, J.S. and Isaksen, I. S. A. 1992. Chemical-dynamical modelling of the atmosphere with emphasis on the methane oxidation, *Ber. Bunsenges. Phys. Chem.*, 96, 241-251.

Crutzen, P.J. 1987. Role of the tropics in atmospheric chemistry. In: *The Geophysiology of Amazonia,* (ed. R.E. Dickinson). John Wiley, New York, 107-130.

Crutzen, P.J. and Zimmermann, P.H. 1991. The changing photochemistry of the troposphere, *Tellus, 43AB,* 136-151.

DeMore, W. B., Margitan, J.J., Molina, M.J., Watson, R.T., Golden, D.M., Hampson, R.F., Kurylo, M.J., Howard, C.J. and Ravishankara, A.R. 1985. Chemical kinetics and photochemical data for use in stratospheric modeling. *Jet. Propul. Lab. Publ., 85-37,* California Institute of Technology, Pasadena.

DeMore, W.B., Sander, S.P., Golden, D.M., Hampson, R.F., Kurylo, M.J., Howard, C.J., Ravishankara, A.R., Kolb, C.E. and Molina, M.J. 1992. Chemical kinetics and photochemical data for use in stratospheric modeling, *Jet. Propul. Lab. Publ. 92-20,* California Institute of Technology, Pasadena.

Dütsch, M. U. 1974. The ozone distribution in the atmosphere, *Can. J. Chem.*, 52, 1491-1504.

Finlayson-Pitts, B.J. and Pitts, J.N. 1986. *Atmospheric chemistry; Fundamentals and experimental techniques.* John Wiley & Sons, New York, 1986.

Fuglestvedt, J.S., Berntsen, T.K. and Isaksen, I.S.A. 1993. Responses in tropospheric O_3, OH and CH_4 to changed emissions of important trace gases. *Report 1993:4,* CICERO, University of Oslo.

Gery, M.W. 1989. Tropospheric air quality. In: *Environmental Effects Panel Report* (eds. J.C. van der Leun, M. Tevini and R.C. Worrest). Nairobi, Kenya.

Gleason, J. F., Bhartia, P.K., Herman, J.R., McPeters, R., Newman, P., Stolarski, R.S., Flynn, L., Labow, G., Larko, D., Seftor, C., Wellenmeyer, C., Komhyr, W.D., Miller, A.J. and Planet, W. 1993. Record low global ozone in 1992. *Science, 260,* 523-526.

Henderson-Sellers, A. and McGuffie, K. 1987. *A climate modelling primer.* John Wiley. Chichester.

Hesstvedt, E., Hov, Ø. and Isaksen, I.S.A. 1978. Quasi steady-state approximation in air pollution modelling: Comparison of two numerical schemes for oxidant prediction. *Int. J. Chem. Kin.,10,* 971-994.

Hidalgo, H. and Crutzen, P.J. 1977. The tropospheric and stratospheric composition perturbed by NO_x emissions from high-altitude aircraft. *J. Geophys. Res., 82,* 5833-5866.

Hough, A.M. 1991. Development of a two-dimensional tropospheric model: Model chemistry. *J. Geophys. Res., 96,* 7325-7362.

IPCC (Intergovernmental Panel on Climate Change) 1992. Climate change 1992. The Supplementary Report to the IPCC Scientific Assessment. (eds. J. T. Houghton, B.A. Callender and S.K. Varney), *Cambridge University Press,* Cambridge.

Iqbal, M. 1983. An introduction to solar radiation. *Academic Press.*

Isaksen, I.S.A. 1980. The tropospheric ozone budget and possible man-made effects. In: *Proceedings of the Quadrennial International Ozone Symposium, Vol II* (ed. J. London). International Ozone Commission, Boulder, CO, Aug. 1980, 845-852.

Isaksen, I.S.A., Midtbø, K.H., Sunde, J. and Crutzen, P.J. 1977. A simplified method to include molecular scattering and reflection in calculation of photon fluxes and photodissociation rates. *Geophys. Norv., 31,* 11-26.

Isaksen, I.S.A., Hov, Ø., Penkett, S.A. and Semb, A. 1985. Model analysis of the measured concentration of organic gases in the Norwegian Arctic. *J. Atmos. Chem., 3,* 3-27.

Isaksen, I.S.A, and Stordal, F. 1986. Antarctic ozone depletion: 2-D model studies, *Geophys. Res. Lett.,13,* 1327-1330, 1986.

Isaksen, I. S. A. and Hov, Ø. 1987. Calculations of trends in the tropospheric concentrations of O_3, OH, CO, CH_4 and NO_x. *Tellus, 39B,* 271-283.

Isaksen, I.S.A. 1988. Is the Oxidizing capacity of the atmosphere changing? In: *The Changing Atmosphere,* (eds. F.S. Rowland and I.S.A. Isaksen) Wiley-Interscience, 141-157.

Isaksen, I.S.A., Berntsen, T. and Solberg, S. 1989. Estimates of past and future tropospheric ozone changes from changes in human released source gases. In: *Proceedings of International Ozone Symposium 1988.* 576-579. A. Deepak publishing. Virginia USA.

Isaksen, I. S. A., Rognerud, B., Stordal, F., Coffey, M.T. and Mankin, W.G. 1990. Studies of arctic stratospheric ozone in a 2-D model including some effects of zonal asymmetries, *Geophys. Res. Lett., 17,* 557-560.

Isaksen, I.S.A., Lee, Y.-P., Atkinson, R., Sidebottom, H., Fuglestvedt, J.S., Johnson, C., Lelieveld, J. and Thompson, A. 1992: Chapter 5: *Tropospheric processes: Observations and interpretation.* Scientific Assessment of Ozone Depletion: 1991, World Meteorological Organization, Global Ozone Research and Monitoring Project, Report No. 25, 1992.

Jonson, J. E. and Isaksen, I.S.A. 1991. The impact of solar flux variations on the tropospheric ozone chemistry. *Institute Report nr. 81.* Institute of Geophysics, University of Oslo.

Jonson, J.E. and Isaksen, I.S.A. 1993: Tropospheric ozone chemistry. The impact of cloud chemistry. *J. Atmos. Chem., 16,* 99-122.

Jonson, J.E. and Isaksen, I.S.A. 1994. The sensitivity of tropospheric chemistry to cloud interactions. To be published in *Proceedings of the 5'th Quadrennial Ozone Symposium,* 1992.

Kanakidou, M. and Crutzen, P.J. 1992. Scale problems in global tropospheric chemistry modelling: Comparison of results obtained with a three-dimensional model, adopting longitudinally uniform and varying emissions of NOx and NMHC. *Chemosphere, 26,* 798-801.

Khalil, M.A.K., Rasmussen, R.A. and Shearer, M.J. 1989. Trends of atmospheric methane during the 1960s and 1970s. *J. Geophys. Res., 94,*18279-18288.

Lelieveld, J., Crutzen, P.J. and Rodhe, H. 1989. Zonal average cloud characteristics for global atmospheric chemistry modelling. *GLOMAC-report UDC 551.510.4, CM 76,* International Meteorological Institute in Stockholm.

Lelieveld, J. and Crutzen, P.J. 1990: Influences of cloud photochemical processes on tropospheric ozone. *Nature, 343,* 227-233.

Lelieveld, J. and Crutzen, P.J. 1991: The role of clouds in tropospheric photochemistry. *J. Atmos. Chem., 12,* 229-267.

Liu, S.C. and Trainer, M. 1988: Responses of the tropospheric ozone and odd hydrogen radicals to column ozone change. *J. Atmos. Chem., 6, 221-233.*

Lloyd, A.C., Atkinson, R., Lurmann, F.W. and Nitta B. 1983. Modeling potential ozone impacts from natural hydrocarbons. I: Development and testing of a chemical mechanism for the NOx-air photoxidations of isporene and α-pinene under ambient conditions. *Atmos. Environ., 17,* 1931-1950.

London, J. and Liu, S.C. 1992. Long-term tropospheric and lower stratospheric ozone variations from ozonesonde observations. *J. Atmos. Terr. Phys.,* 54, 599-625.

Madronich, S. 1987. Photodissociation in the atmosphere. 1: Actinic flux and the effect of ground reflection and clouds. *J. Geophys. Res., 92,* 9740-9752.

Madronich, S. 1993. Tropospheric photochemistry and its response to UV changes. In: *The role of the Stratosphere in Global Change* (ed. M.L. Chanin). NATO ASI series, Vol. I 8, 437-461, Springer-Verlag Co. Heidelberg.

Madronich, S. and Calvert, J.G. 1990. Permutation reactions of organic peroxy radicals in the troposphere. *J. Geophys. Res., 95,* 5697-5715.

Madronich, S. and Granier, C. 1992. Impact of recent total ozone changes on tropospheric ozone photodissociation, hydroxyl radicals, and methane trends. *Geophys. Res. Lett., 19,* 465-467.

Müller, J.-F. 1992. Geographical distribution and seasonal variation of surface emissions and deposition velocities of atmospheric trace gases. *J. Geophys. Res., 97,* 3787-3804.

Newell, E., Kidson, J.W., Vincent D.G. and Boer, G.J. 1972. The general circulation of the tropical atmosphere and interactions with extratropical latitudes. M.I.T. Press, Cambridge, Mass., Vol. 1.

Schnell, R. C., Liu, S.C., Oltmans, S.J., Stone, R.S., Hofmann, D.J., Dutton, E.G., Deshler, T., Sturges, W.T., Harder, J.W., Sewell, S.D.,Trainer, M. and Harris, J.M. 1991. Decrease of summer tropospheric ozone concentrations in Antarctica, *Nature, 351,* 726-729.

Smolarkiewicz, P.K. 1983. A simple positive definite advection scheme with small implicit diffusion. *Am. Met. Soc., 111,* 479-487.

Stordal, F., Isaksen, I.S.A. and Horntveth, K. 1985. A diabatic circulation two-dimensional model with photochemistry: Simulations of ozone and long-lived tracers with surface sources. *J. Geophys. Res., 90,* 5.757-5.776.

Sze, N.D. 1977. Anthropogenic CO emissions: Implications for the atmospheric CO-OH-CH_4 cycle. *Science, 195,* 673-675.

Thompson, A.M. 1984. The effect of clouds on photolysis rates and ozone formation in the unpolluted troposphere. *J.Geophys. Res, 89,*1341-1349.

Thompson, A.M. and Cicerone, R.C. 1986. Possible perturbations to atmospheric CO, CH_4 and OH. *J. Geophys. Res., 91,* 10853-10864.

Thompson, A.M., Owens, M.A., Stewart, R.W. and Herwehe, J.A. 1989. Sensitivity of tropospheric oxidants to global chemical and climate change. *Atmos. Environ. 23,* 516-532.

Thompson, A.M., Huntley, M.A. and Stewart, R.W. 1990. Perturbations to tropospheric oxidants, 1985-2035: 1. Calculations of ozone and OH in chemically coherent regions. *J. Geophys. Res., 95,* 9829-9844.

Thompson, A.M. 1991. New ozone hole phenomenon. *Nature, 352,* 282-283.

Vaghjiani, G.L. and Ravishankara, A.R. 1989. Kinetics and mechanism of OH reaction with CH_3OOH. *J. Phys. Chem, 93,* 1948-1959.

Vaghjiani, G.L. and Ravishankara, A.R. 1991. New measurements of the rate coefficient for the reaction of OH with methane. *Nature, 350,* 406-409.

Valentin, K. 1991. Numerical modelling of climatic and anthropogenic influences on global atmospheric chemistry since the last glacial maximum. *Ph.D. thesis,* University of Mainz, Germany.

Watson, R.T., Kurylo, M.J., Prather, M.J. and Ormond, F.M. 1990. Present state of knowledge of the upper atmosphere 1990: An assessment report. *Report to congress.* NASA reference publication 1242.

WMO (World Meteorological Organization) 1992. Scientific assessment of ozone depletion: 1991, *WMO/UNEP Global Ozone Research and Monitoring Project,* Report No. 25, Geneva.